ADDIS ABABA UNIVERSITY

ADDIS ABABA INSTITUTION OF TECHNOLOGY

Design and Modification of Appropriate Reel Mechanism to Harvest Tef Crop

by

Ephrem Zeleke

a Thesis

Submitted in Partial Fulfillment of the Requirement for

The Master of Science Degree

in

Mechanical Engineering
(Mechanical Design)

Advisor

Dr.-Ing. Zewdu Abdi

October, 2012

Design and Modification of Appropriate Reel Mechanism to Harvest Tef Crop

Acknowledgement

I am grateful to individuals and organizations that have helped me in different but valuable ways in the preparation of this thesis. I first and foremost owe a special debt of gratitude to my advisor Dr:-Ing Zewdu Abdi, who helped me by giving some wise comments and idea. I also want to acknowledge Mr. Hailu Luche and Mr. Mekasha from the Caleb Farmer's House who gave me data, materials and some very useful advises. Special thanks are to Addisu Negash and Abdulhakim Shukurea who helped me by giving me different idea and materials.

Abstract

The relationships between the deflection angle and deflection force acting on a bunch of crop stalk in the gathering operations of a combine harvester reel were analyzed. Mechanical crop model based on bending theory with regard to an elastic beam were applied in this analysis. In the model, the effect of flexural rigidity, crop ear weight and reel force on tef crop stalk in the angle of deflection. A model of crop stem deflection by the combine harvester reel is formulated. The equations derived thereof are evaluated on the basis of empirical data that were acquired through deflection of crop stems in a ready for harvest tef crop in the field. Applications of crop stem deflection to reel design and operation are used for determination of the number of reel tine bar and angular displacement of successive tine bar. The reel design includes determination of the number of tine bar, angular displacement of the reel and rotational speed of reel. The reel adjustment forward and backward relative to the cutter bar and also height adjustment appropriate to the tef crop height. The design of chain derives, shaft and bearing took varies data with appropriated values from the actual combine harvester such as reel speed and maximum torque. In chain drive design, the diameter of larger sprocket and the length of chain were calculated. In shaft design, determination of diameter of shaft that holds the reel force and sprocket tangential force by selected material. In bearing selection, calculating basic dynamic load rating was made to determine type of bearing number, then the correct bearing selected.

Table of Contents

List of Figures

List of Table

Notation

M	Bending moment, N mm
I	Second moment of area, mm^4
E	Modulus of elasticity, N/mm^2
ρ	Radius of curvature, mm
D	Flexural rigidity, N mm^2
l_e	Length of an ear, mm
l_c	x coordinate of centre of an ear, mm
l	Length of a crop stalk, mm
P	Reel force, N
R	Radius of the reel, mm
t	Time, s
u	Peripheral speed of the reel, mm/s
W	Weight of an ear, N
V_m	Forward speed of the machine, mm/s
x, y	Global coordinates, mm
x_p, h_p	x, y coordinates at loading point, mm
x_t, h_t	x, y coordinates at the tip of a crop stalk, mm
ω	Angular velocity of the reel, rad/s
θ_t	Deflection angle at the tip of the crop stalk, rad
φ	Angular deformation of the deflected cantilever, rad
α	Angular displacement between successive tine bars, rad
h_r	Height of the axis of the reel above the ground, mm
Z_r	Reel stagger, mm
R_0	Distance whose magnitude is equal to header advance per radian of reel rotation, mm
T	Torque, Nm
N	Speed of rotation, rpm
C	The basic dynamic load rating, kN
d	Diameter of shaft, mm
L	Length of chain, m

1. Introduction

1.1. Background of study

Tef is among Ethiopia's most important cereal crops. It is indigenous to the country and part of the culture, tradition and food security of its people. The crop is grown over approximately 2.8 million hectares or 27% of the land area under cereal production CSA, (1999). Tef is endemic to Ethiopia and its major diversity is found only in this country. According to Ponti, (1978) tef was introduced to Ethiopia well before the Semitic invasion of 1000 to 4000 BC.

Tef is nutritionally rich it has very high calcium content, and contains high levels of phosphorous, iron, copper, aluminium, barium, and thiamin. It is considered to have an excellent amino acid composition, with lysine levels higher than wheat or barley and slightly less than rice or oats Stallknecht, (1997). Tef is high in protein, carbohydrates, and fiber. The protein composition offers an excellent balance among the essential amino acids Yu et al., (2006). Teff grains and flour do not contain gluten and are rich in minerals, especially iron Spaenij-Dekking et al., (2005).

Tef is an annual tufted grass, 25 – 135 cm high, with slender culms and long, narrow, smooth leaves. It is shallow-rooted. Its inflorescence is a loose or compact panicle (11 – 63 cm length) Dawit and Hirut, (1995).

Tef crop will be threshed well with standard methods and equipment and harvested when the vegetative parts turn yellowish. This depends on the maturity period of the varieties, which varies very early maturing types are ready to harvest in 45 – 60 days; early types in 60 – 120 days; and late types in 120 – 160 days Tefera et al., (1995). Harvesting before the plant gets too dry helps prevent losses from shattering. It is threshed by trampling the harvested crop either with oxen or by using threshers. The grain is stored outside the house in a granary made of wood or bamboo plastered with mud mixed with tef straw to reinforce it, or stored in the house using other storage containers.

The seeds are so small that this alone makes the crop hard to deal with. The fields are tedious to prepare, and it is difficult to get an even stand. Also, wind or rain can bury the minute seedling before it can establish itself. Threshing, winnowing, and grinding such tiny seeds by hand is very

laborious. Stationary threshers or combine harvesters are used to thresh tef. However, seed loss is incurred because tef seed is very small and light and gets blown away with the chaff. Harvesting of the crop is difficult because of lodging. Since tef lodges heavily it is not advisable to use higher rates of fertilizer to increase yield Seyfu, (1997). The current landraces and cultivars used are not lodging resistant and the development of genetically lodging-resistant cultivars is essential.

The combine harvester is a machine that harvests grain crops and is widely used in precision farming. It combines into a single operation a process that previously required three separate operations (reaping, binding, and threshing). Among the crops harvested with a combine are wheat, oats, rye, barley, corn (maize), soybeans, and flax (linseed). Combines are equipped with removable heads that are designed for particular crops.

Combine harvesters equipped with the right attachments can harvest grains and seeds of a wide range of types and sizes, from mustard seeds to broad beans, from ground hugging clovers to corn over 2m tall. They recover the grains from the field and separate them from the rest of the crop material, the *material other than grain* (MOG), which is dumped back on the field. Since the transition from hand harvest to the use of combine harvesters, productivity of harvesting has increased from 10 kg/man-hour in 1800 to about 60,000 kg/man-hour with stripper header today and losses are reduced to as low as 1% – 3%. Different crop properties and different harvest conditions make great demands on combines. The combine has to match these demands by design, and the driver has to continually adjust the combine to the optimum for each crop and harvest condition.

The main processes in a modern combine harvester are gathering and cutting, threshing, separating, cleaning, and materials handling. The main elements of a conventional combine with straw walkers.

- The header (cutting platform) divides, gathers and cuts the crop with a reel and cutter bar then augers the crop into the feeder house for presentation to the threshing unit.
- The threshing unit consisting of threshing drum and concave (sometimes with additional accessories), which detach the grain from the ears.
- The separator unit or straw walker separates the remaining grain from the straw.

- The cleaning unit does the final separation of grain from the chaff and broken straw pieces delivered by the concave and straw walker. The clean grain is conveyed into the grain tank. Unthreshed grain heads or pieces of cob (tailings) are returned for rethreshing.

Fig. 1 Combine harvester header (cutting platform)

Apart from self-propelled combines, there is a small market for pull-type combines and a few tractor-mounted combines. These are powered by PTO drive, and are either tractor drawn or affixed onto the tractor. Since they need no separate engine, drive train or operator compartment, these combines are cheaper, but have some major disadvantages, such as: restricted view of the header, less maneuverability, and lower speed, depending on the tractor available. More preparation time is required than for self-propelled combines and the pulling tractor is unavailable for other work. In hilly areas, there are specially built hillside combines on the market, which keep the harvester body level on slopes of 10% – 12% by adjusting the drive axle as well as the rear steering axle.

The reel controls feeding of the upper part of plants into the grain platform. Bats on the reel push the top of plants over the cutter bar to aid cutting and sweep the material across the platform. For soybean or rice crops, pick-up fingers are often added to the reel to help lift and pick up lodged crop. The center of the reel is slightly ahead of the cutter bar. If pick-up fingers are used, the reel should be positioned so that fingers clear the cutter bar by at least 1 inch for all conditions (also in the uppermost flexed position of flexible cutter bars).

Peripheral reel speed should be slightly faster than ground speed in good harvesting conditions. The dimensionless ratio of peripheral reel speed to ground speed is the reel index. An average setting is about 1.25, but reel speed controllers should have the ability to vary the reel index from about 1.1 to 2.0, with faster speeds being used to more aggressively gather lodged crop into the head.

1.2. Statement of Problem

The tef crop has naturally lodging property than other crops such as rice and wheat so it is difficult to reel and cut the crop by combine harvester or other harvester. During harvesting tef using combine harvester the tef grain losses can be high due to the interaction between the reel and crop as the crop is thinner, shorter and lodges easily. The purpose of this thesis is harvesting the tef crop with minimum losses of the tef grain during taking the crop for the purpose of cutting that is reduced losses of the tef grain by harvester reel.

1.3. Objective

The objective is to understand crop stem deflection characteristics, under the action of the combine harvester reel, and to apply these characteristics in combine harvester reel design and operation.

General objective

- Design and/or modification of combine harvester reel mechanism to harvest tef crop

Specific objective

- Tef crop's mechanical and physical properties will be investigated
- Determine reaction force by reel on the tef crop will be measured
- Design or modification of the reel of the harvester

2. Literature Review

The reel in a combine harvester machine delivers the stalks to the cutting mechanism, holds them upright during cutting and pushes the cut crop towards the platform conveyor. Pickup reels are used for lodged crops (crops that have fallen over due to heavy rains, winds, etc.), because they have fingers that reach into the lodged crops and help pick them up for cutting.

Optimum reel position is determined by the crop height, amount of straw cut, and the condition of the straw. Normally, the reel should be set so the slats, when in their lowest position, will strike the straw 15 to 25 cm above and slightly ahead of the cutterbar (Srivastava el.al, 1993). For lodged crops the reel should be set farther back. Proper reel speed is important to minimizing shattering and gathering losses. A reel turning too fast will result in excessive shatter loss, whereas too slow speed will result in the cut grain head falling off the platform, a cutterbar loss.

In Ethiopia, lodging of tef is also a common phenomenon and one of the causes for the current low grain yields: the Ethiopian national average grain yield of tef is in the order of 800 kg ha^{-1} (Tulema et al., 2005). This low national average is partly associated with constraints such as water logging, drought and nutrient limitation (Tulema et al., 2005). The yield of well-fertilized unsupported plants in 'on station' field experiments is, on average, in the order of 2500 kg ha^{-1} (Tulema et al., 2005). However, Teklu & Tefera (2005) reported yields up to 4600 kg ha^{-1} for tef supported with nets to prevent lodging. The difference in yield between naturally growing tef and supported tef implies that solving tef's lodging problems would dramatically increase actual yield. Lodging resistance, therefore, is the main focus in several breeding programmes (Yu et al., 2006).

Crook & Ennos (1994) developed simple equations to investigate lodging phenomena in cereals. These static equations predict a relative degree of susceptibility to anchorage failure and shoot failure, known as root and shoot lodging, respectively. According to Crook & Ennos (1994), lodging susceptibility in cereals depends on three factors: first, the size and dynamics of the forces to which the plant is subjected (Pinthus, 1974); second, the bending strength of the shoot and its resistance to buckling; and third, the anchorage strength of the root system. Although the static equations developed by Ennos and coworkers only take the second and third factors into account, while neglecting influences by wind, the results corresponded well with field

observations Crook & Ennos (1994). Yet, these equations do not aim to predict the actual onset of lodging in the field as a result of weather conditions (Baker et al., 1998).

Bultosa and Taylor (2004) commented on the possibility of using a combine harvester for harvesting of tef, but they added that tef grain losses can be high due to the very small size and light mass of the grain. The equivalent diameter of tef grain was reported to vary between 0.71 and 0.87 mm and thousand grain mass 0.257–0.421 g in the moisture content range 5.6 % to 29.6 % w.b. (Zewdu & Solomon, 2007). Tef was said to have a prolate spheroid shape, which results in its dimensions being represented by a length and diameter. The sphericity of tef varies between 0.6 and 0.7 (Zewdu & Solomon, 2007).

For agricultural machines, it would be advantageous to assess performance of the machine taking the crop properties into account at the design stage instead of through actual machine tests, especially from the view points of cost reduction, shortening of the development period, and clarification of optimum machine operations according to crop conditions. In order to improve the process of design and development, investigations of physico-mechanical properties and behaviour of crops caused by machine operations are important, and also lead to development of analytical techniques simulating the harvesting process. The reaction force of a tef stalk undergoing forced displacement was investigated based on a mechanical model of a crop stalk. It is similar to the mechanical response of a crop stalk during gathering operations by the combine harvester reel, and is also important information to clarify lodging phenomenon.

Several investigators have studied a variety of physico-mechanical properties of biological materials for the purpose of applying them to machine design, mechanical processes and lodging problems (Inoue et al., 1998). A large deflection equation for an elastic beam was applied to a rice stalk, and the relevance of this to large deflections of crop stalks was discussed based on a mechanical model of a crop stalk (Inoue et al., 1998). A mechanical model of a crop stalk with a heterogeneous cross-section was proposed, based on bending theory for an elastic beam (Timoshenko, 1940), and also a calculation method of flexural rigidity for materials with a heterogeneous cross-section was inspected by deflection tests using piano wire (Hirai et al., 2002a). An extended model that takes into account the effect of a crop ear was proposed, and the relationships between the deflection and deflection force (horizontal force component) acting on a bunch of crop stalks were analyzed under a standing crop condition (Hirai et al., 2002a). The

effects of frictional force and the vertical force component were considered, and horizontal and vertical reaction forces on the bunch of crop stalks were analyzed under a standing crop condition utilizing a differential equation describing deflection (Hirai et al., 2002b). It was determined that the equation was useful for investigating the deflection characteristics, and also that the analytical accuracy of the reaction force would be increased by considering the effect of the initial shape of individual crop stalks.

Differences in the tendencies of the reaction forces due to the initial shape of a wheat stalk have previously been investigated (Hirai et al., 2003a), and a differential equation describing deflection, taking into account the initial shape of wheat stalk, was derived based on a mechanical model of a crop stalk. Reaction forces of a single wheat stalk undergoing forced displacement were accurately predicted utilizing the derived equation, and the subsequent application of the derived equation to a bunch of wheat stalks was also verified by experiment (Hirai et al., 2003b).

The gathering performance of a combine harvester reel is affected by the control or design parameters such as height and speed index of the reel, and the setting of the axis of the reel relative to the knife bar (Srivastava et al., 1993), and these parameters are adjusted according to crop conditions. Thus, the investigations of the mechanical responses of crop stalk during the gathering operation are important to provide more effective control under specific crop conditions and to develop a control system, which offers stable performance and reduces the burden on the operator. Further, theoretical clarification of the mechanical response of crop stalk leads to the development of the analytical techniques simulating the harvesting process, which contributes to cost reduction and the shortening of the development period (Hirai et al., 2002a).

The reel operation have mainly shown the geometric motion of the reel and the results of a laboratory and field test Oduori et al., (1993); Oduori, (1994), while the general design standard to assess the gathering performance has not been developed because the reel–crop interaction was not considered theoretically. Thus, Inoue et al., (1998) have investigated mechanical properties of the crops, such as flexural rigidity and frequency response (Inoue et al., 1998), and the mechanical responses the crops, such as the reaction force and deflection shape (Hirai et al., 2002a, 2002b), in order to clarify the reel–crop interaction related to the gathering performance. Further, the authors have developed the analytical method for the determination of the reaction

force and deflection shape of the crop stalks undergoing forced displacement based on a mechanical model of a crop stalk, because the basic operation of the reel prior to cutting crops is to deflect crop stalks by the rotational motion. The analytical method for the determination of the reaction force has been verified for a single wheat stalk (Hirai et al., 2003a), a bunch of wheat stalk (Hirai et al., 2003b), under a quasi-static loading condition.

Further, the model was also used for posture analysis. The change of the crop posture due to the reel operations causes a change in the centre of gravity of the crop stalk, which significantly affects the motion of the cut stalk. For the analysis of crop posture: load (deflection force), height at the loading point, and the physical properties of crops, such as flexural rigidity are required data. In the case of a standing crop stalk, deflection of the crop stalk at the reel acting point (loading point) is determined geometrically. When the deflection force at the reel acting point, which varies with the reel trajectory of a trochoid, is consistently predicted based on the deflection determined at the loading point in the crop model, the model is demonstrated to be applicable to posture analysis. From the above reasons, the relationships between deflection and deflection force were measured through a series of experiments involving reel operations, and the application of the mechanical model to the investigation of the reel crop interaction and the analytical methods of determining deflection force were evaluated by comparing the results.

The purposes of a reel are to hold the crop against the cutting mechanism, to clear the cut stalks from the cutter, and to deliver cut material to other working units of the machine Kepner et al., (1972). Its effectiveness is dependent upon the path of the edge of the bats; the closer they pass to the cutter the better the clearing of cut material and the more constant the feed rate. The speed index is the ratio of reel peripheral speed to machine forward speed. Kepner et al. (1972) recommended an index of 1.25 to 1.50 for standing crops. Higher ratios may be more effective in moving material back from the cutter but tend to increase shatter losses in grain. Richey (1961) recommended indices of 1.1 to 3.4 for a 1.1 m (42 in.) diameter reel operating over a range of ground speeds.

The three types of reels commonly used on agricultural harvesting machinery are fixed-bat, pick-up, and copying reel (Klenin et al., 1970). Fixed-bat reels are the simplest and least expensive, consisting of a rotating shaft with 4 to 8 bats rigidly mounted on radial arms (Kepner et al., 1972). They work best in standing crops. Lodged crops can be partially recovered by using a pick-up reel (Richey, 1961) usually equipped with spring teeth on hinged bats. An eccentric adjustment changes the bat angle so the teeth can be angled to pick up the downed crop. The pick-up reel also operates well in standing crops when the bats are adjusted to remain vertical Kepner et al., (1972). The copying reel has bats attached to a cam controlled carrier which causes them to execute a complex motion. This reel can operate close to both the cutter and subsequent working units, keeping the cutter clear and providing a uniform feed rate (Klenin et al., 1970).

3. Methodology

- Surveying different literature (journals and books) about the tef crop posture of standing, deflection and force of deflection and combine harvester reel.

- The tef crop physical properties such as crop height, panicle length and era weight measured.

- Mechanical properties such as flexural rigidity (modulus of elasticity and second moment of inertial) were investigated.

- Mechanical models were formulated that are used to determine the relationships between deflection and the deflection force acting on a bunch of crop stalks, with a purpose investigating the mechanical interactions that take place in gathering operations prior to cutting the crops. The deflection force is a useful data for estimating power requirements for reel operations according to a variety of crop conditions, such as the physical properties of the crop, crop posture, and plant spacing.

- Models were formulated that are used to determination of relationships between reel stagger, angular displacement of successive tine bars and rotational motion of reel. The angular displacement of successive tine bars is a useful data for determining number of reel tine bars.

- Design of reel, shaft, bearing and chain by using analytical method.

4. Mechanical Models of the Tef Crop Stalk

4.1. Deflection of a cantilever beam loaded with a concentrated load

In cantilever beam, when the cantilever is loaded at some point between the ends at a distance a, from the built in support, Figure 5, the beam between G and D carries no bending moments and therefore remains straight. The deflection at G can be (Ross el.al, 1999)

$$\theta_a = \frac{Wa^2}{2EI}, \qquad for\ z = a \qquad \text{Eqn. (4.1)}$$

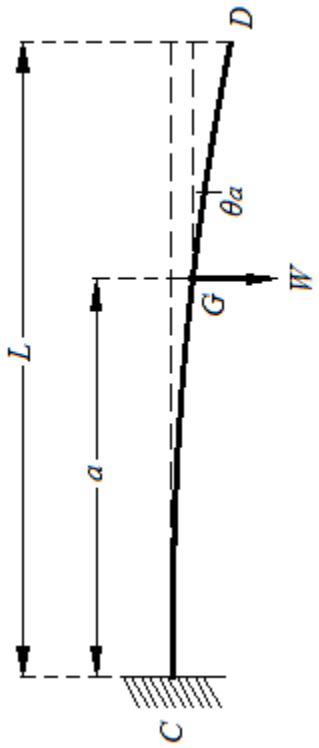

Fig. 5 Cantilever with a load applied between the ends.

4.2. Crop model with homogeneous cross-section and the effect of an ear

The Tef crop stalks takes as initially bent simply supported beam or cantilever beam and reel acting load on with a concentrated load; the deflection force shall be considered to be horizontal and the stress-strain relationship for the deflected stems shall be assumed to be linearly elastic. The assumption of small deflections, commonly made in mechanical and structural engineering,

is not made here. So, there are two different expressions for the bending moment corresponding to the two portions of the crop stalk. The extended crop model that takes into account the effect of an ear under deflection force P at height h_p and θ_t, deflection angle at the tip of a stalk is shown in Fig. 6. In this model, the weight of an ear is added as a concentrated mass of the tip of the stalk. When the effect of a stalk is regarded as a distributed load along its length, its effect on deflection is estimated to be small compared with that of the ear weight because the line density of the stalk decreases toward the tip of the stalk. A simplification of the model is considered as well, with this model not taking into account the effect of the stalk mass.

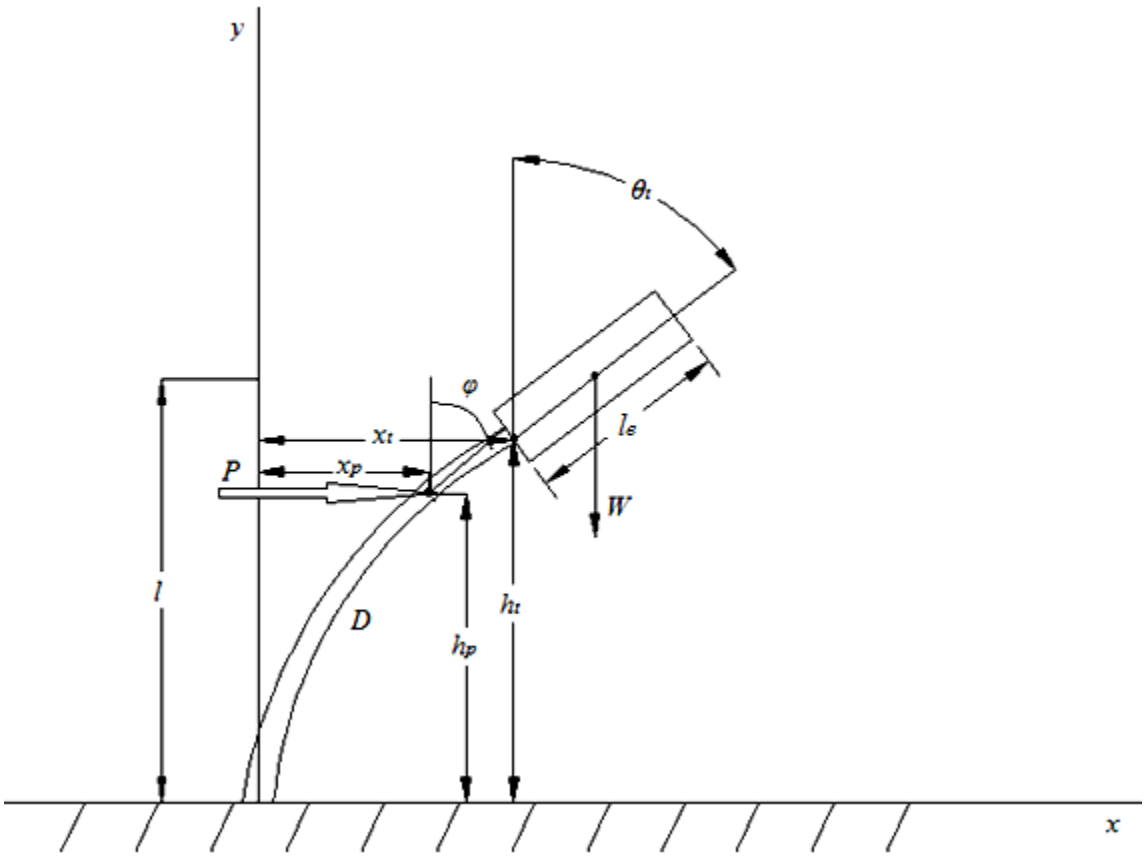

Fig. 6 Extended crop model with the effect of an ear under deflection force P at height h_p

The deflection equation in this model is derived as follows:

a. $0 \le y \le h_p$ or $y \le h_p$

$$\frac{d^2x}{dy^2} = \frac{P(h_p - y) + W(l_e \sin\theta_t/2 + x_t - x)}{EI} \qquad \text{Eqn. (4.2)}$$

b. $h_p \leq y \leq h_t$ or $y \geq h_p$

$$\frac{d^2x}{dy^2} = \frac{W(l_e \sin\theta_t/2 + x_t - x)}{EI} \qquad \text{Eqn. (4.3)}$$

The differential equation describing deflection was derived based on the mechanical model of a crop stalk as shown in Figure 6. The effect of an ear was considered to be a load concentrated at the tip of the stalk. The flexural rigidity *D* was expressed as one parameter, while it was generally expressed as the product of the modulus of the stalk's elasticity and its moment of inertia.

The deflection angle φ of crop with vertical line

$$\varphi = \frac{dx}{dy} = \frac{P\left(h_p y - \frac{y^2}{2}\right) + W(l_c - x)y}{EI} \qquad \text{Eqn. (4.4)}$$

At the ground $y = 0$, there is zero slope in the deflected form, so that $dx/dy = 0$; then the above equation constant gives zero.

$l_c = l_e \sin\theta_t/2 + x_t$ and $(x, y) = (x_p, h_p)$

$$\varphi = \frac{dx}{dy} = \frac{P\frac{{h_p}^2}{2} + W(l_c - x_p)h_p}{EI} = \frac{h_p\left[Ph_p + 2W\left(l_c - x_p\right)\right]}{2EI} \qquad \text{Eqn. (4.5)}$$

Table 1 Data regarding tef crop stalk reel force, flexural rigidity, ear weight, crop length and center length of ear

Reel force, *N*	0.1 – 0.9
Flexural rigidity, *kN mm*^{2}	19.8 – 46.1
Ear weight, *N*	0.020 – 0.039
Crop length, *mm*	250 – 1350
Center length of an ear, *mm*	90 – 690

4.3. Flexural rigidity and Deflection angle

Flexural rigidity has included young's modulus and moment of inertia of the tef crop and the value varies from one crop stalk to another crop, because of different crop diameter and moisture content. By solving eqn. (4.4) in MATLAB, taking the reel force acting the crop and the weight of ear are constant values; calculating deflection angle with varying flexural rigidity. The values below shown in figure 7 are obtained. Therefore, increase flexural rigidity of the crop stalk properties result in decrease of the deflection of the crop stalk as shown in the figure 7.

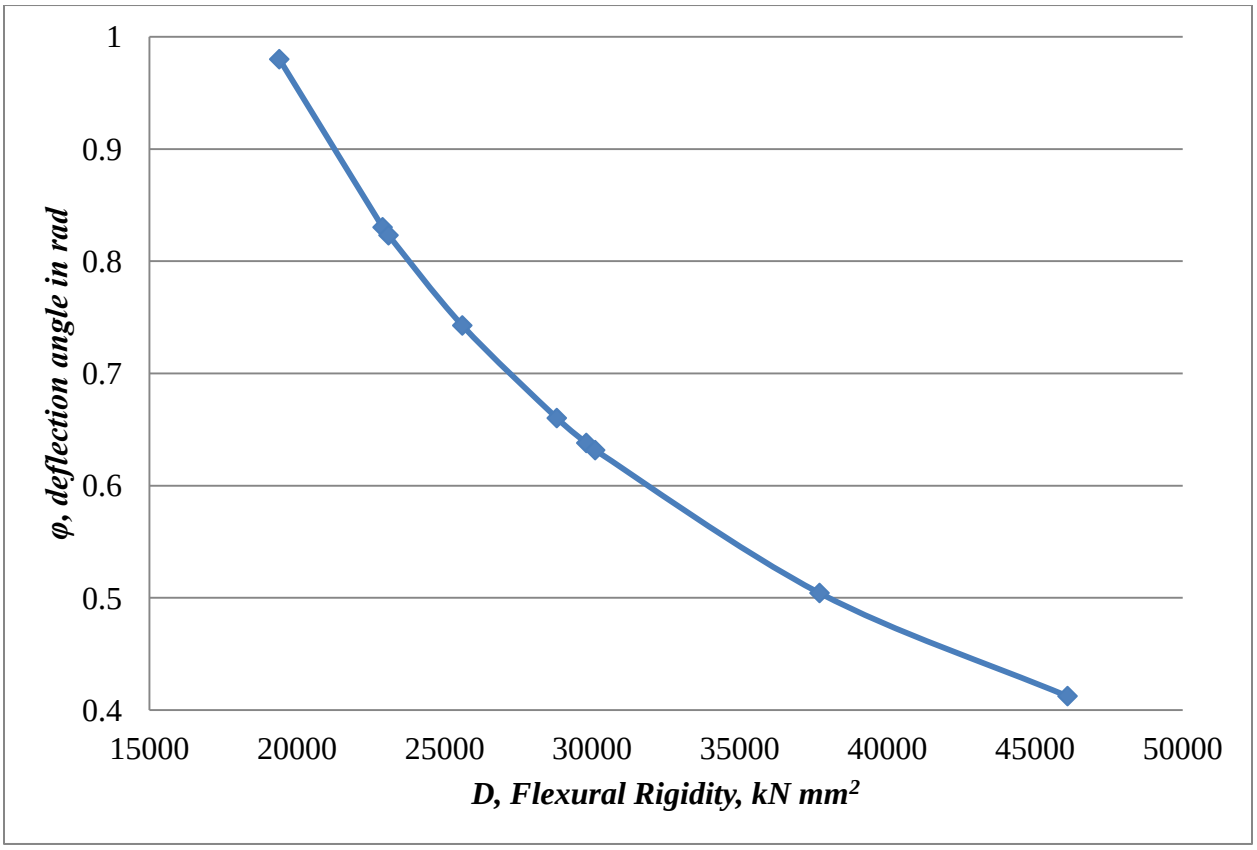

Fig. 7 Effect of flexural rigidity on deflection angle, $P = 0.5\ N$ and $W = 0.025\ N$

4.4. Reel force and deflection angle

The reel force that acts on the crop stalk is directly proportional to the deflection. By solving eqn. (4.4) in MATLAB, taking the flexural rigidity of the crop and the weight of ear as constant values, calculating the deflection angle of the crop stalk by varying the reel force and values below in figure 8 are obtained. The deflection angle increased as reel force increased linearly as shown in figure 8.

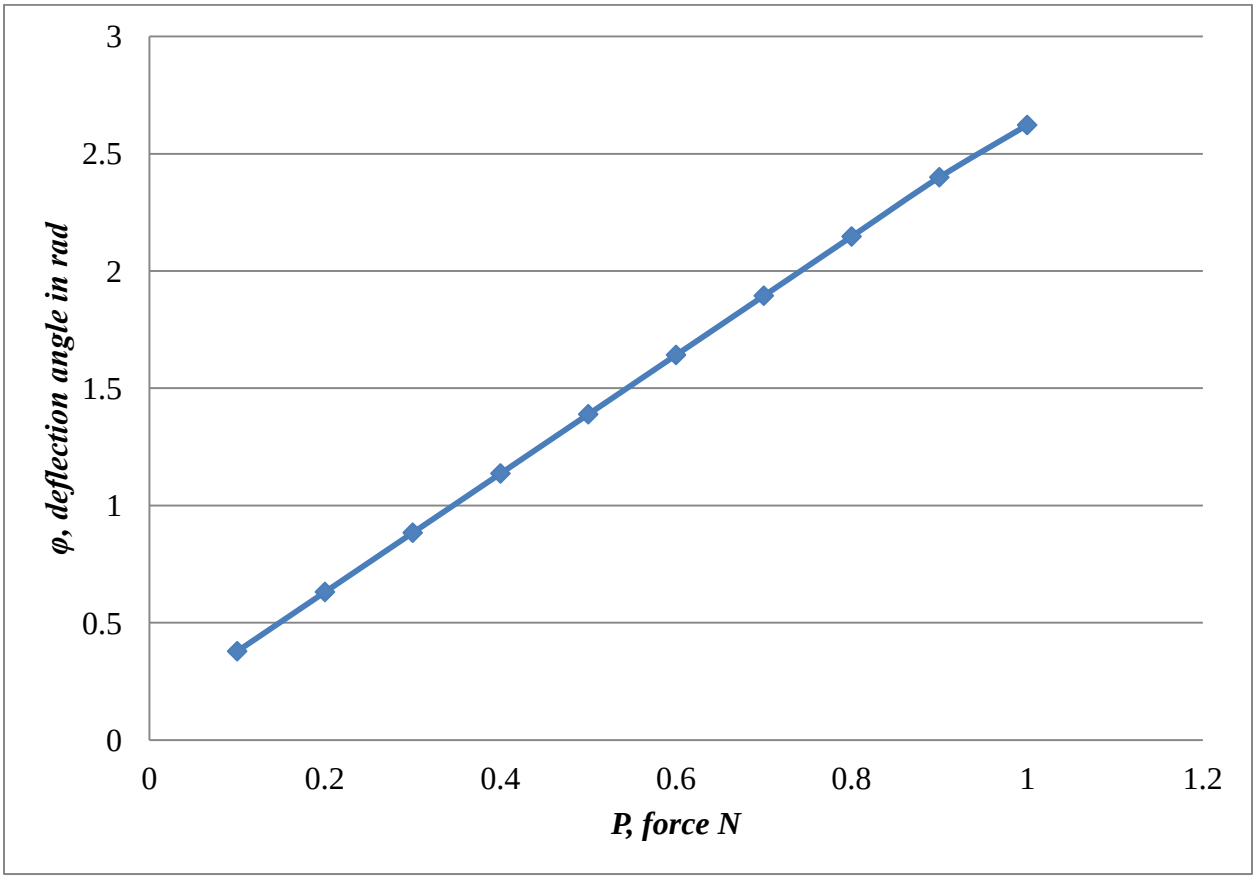

Fig. 8 Effect of reel force on deflection angle, $D = 30.1\ kNmm^2$ and $W = 0.025\ N$

4.5. Weight of ear and deflection angle

The weight of ear varies with length of ear, moisture content and amount of grain. By solving eqn. (4.4) in MATLAB, taking the reel force acting on the crop and the flexural rigidity of crop stalk being constant, the deflection angle vary with varying weight of ear. The deflection angle increased with varying weight of ear as shown in figure 9. Weight of ear has effect on the crop stalk deflection but its effect is small compared to the effect of reel force and flexural rigidity.

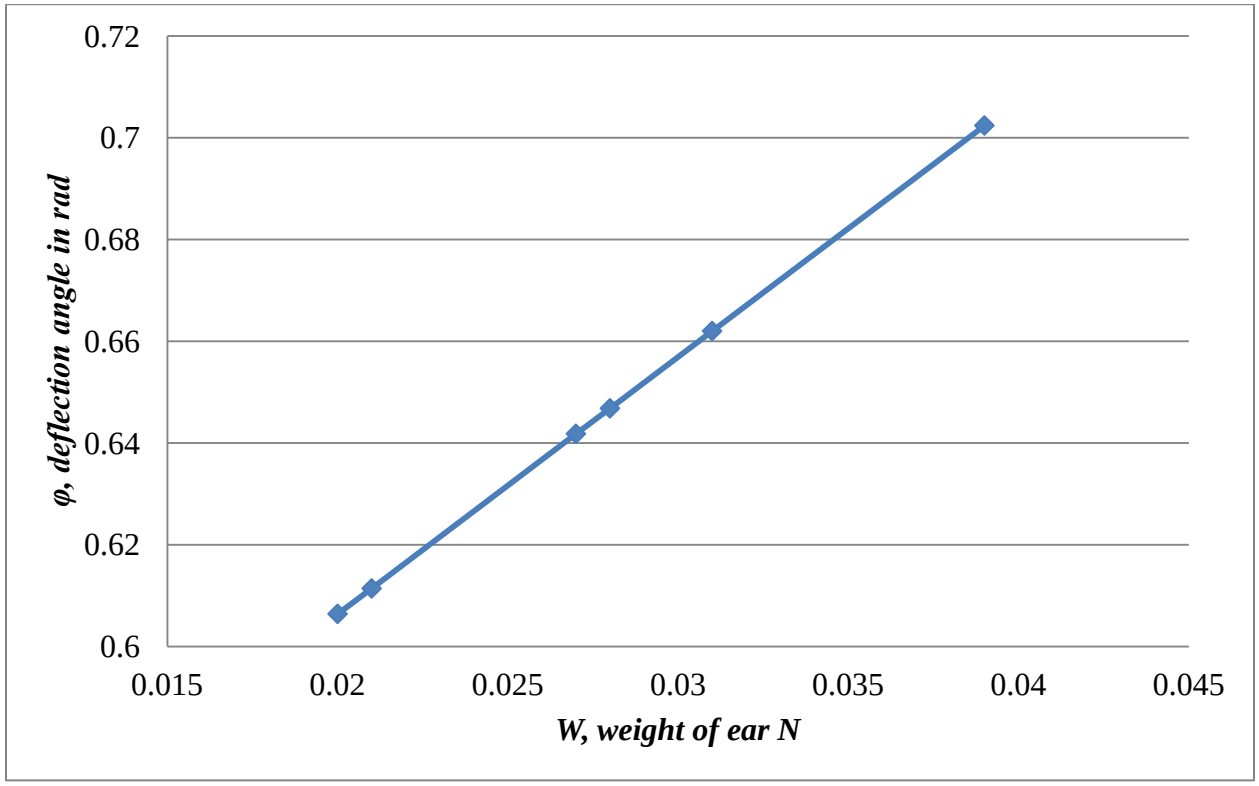

Fig. 9 Effect of weight of ear on deflection angle, $P = 0.5\ N$ and $D = 30.1\ kNmm^2$

4.6. Loading point and deflection angle

Loading point is a point that reel force acts and it depends on the length of tef crop. By solving eqn. (4.4) in MATLAB, taking the reel force acting on the crop, flexural rigidity of crop stalk and weight of ear as constant values, calculating deflection angle of the crop stalk by varying loading point yields values shown in figure 10. The loading point has affected deflection angle.

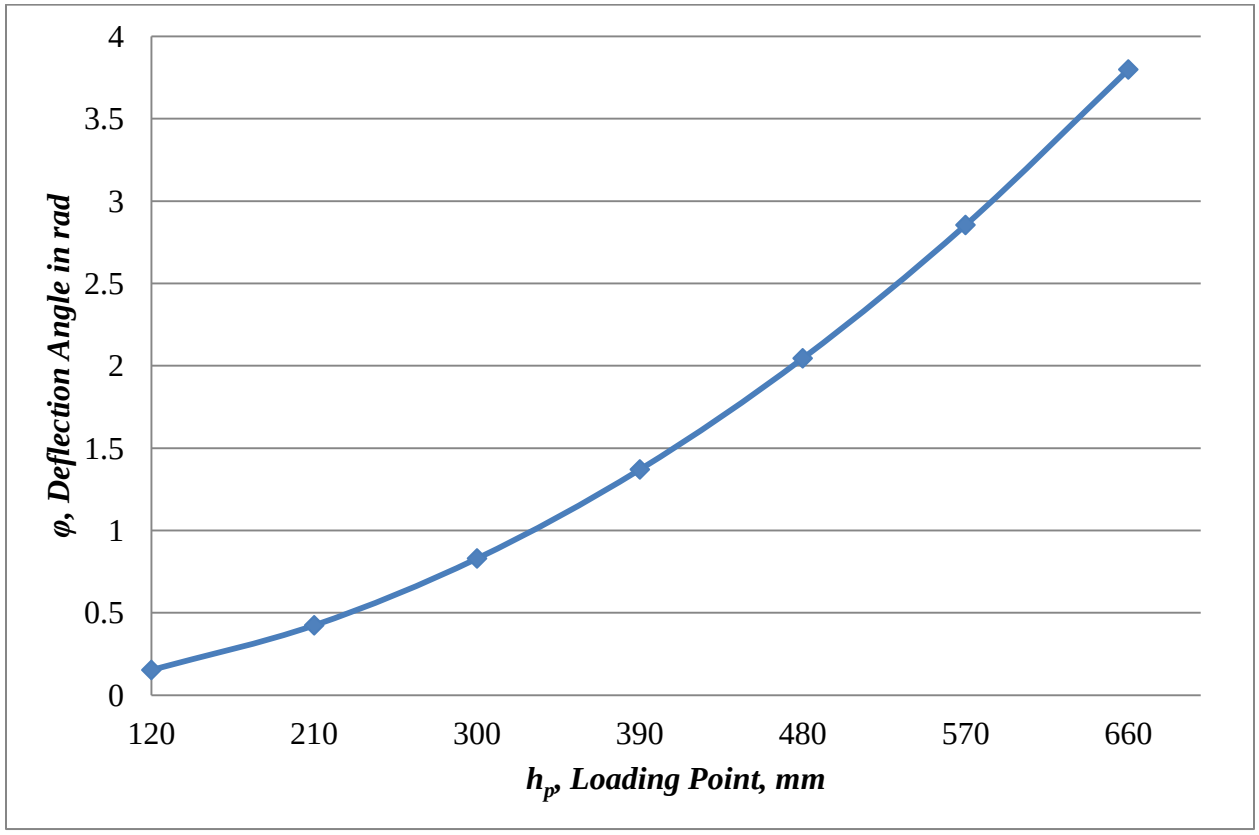

Fig. 10 Effect of loading point on deflection angle, $P = 0.5\,N, D = 30.1\,kNmm^2$ and $W = 0.025\,N$

4.7. Center length of an ear and deflection angle

By solving eqn. (4.4) in MATLAB, taking the reel force acting on the crop and the flexural rigidity of crop stalk and weight of ear as constant values, calculating deflection angle of the crop stalk by varying the center length of an ear yields values below in the graph. The deflection angle slightly increased with varying center length of an ear as shown in figure 11.

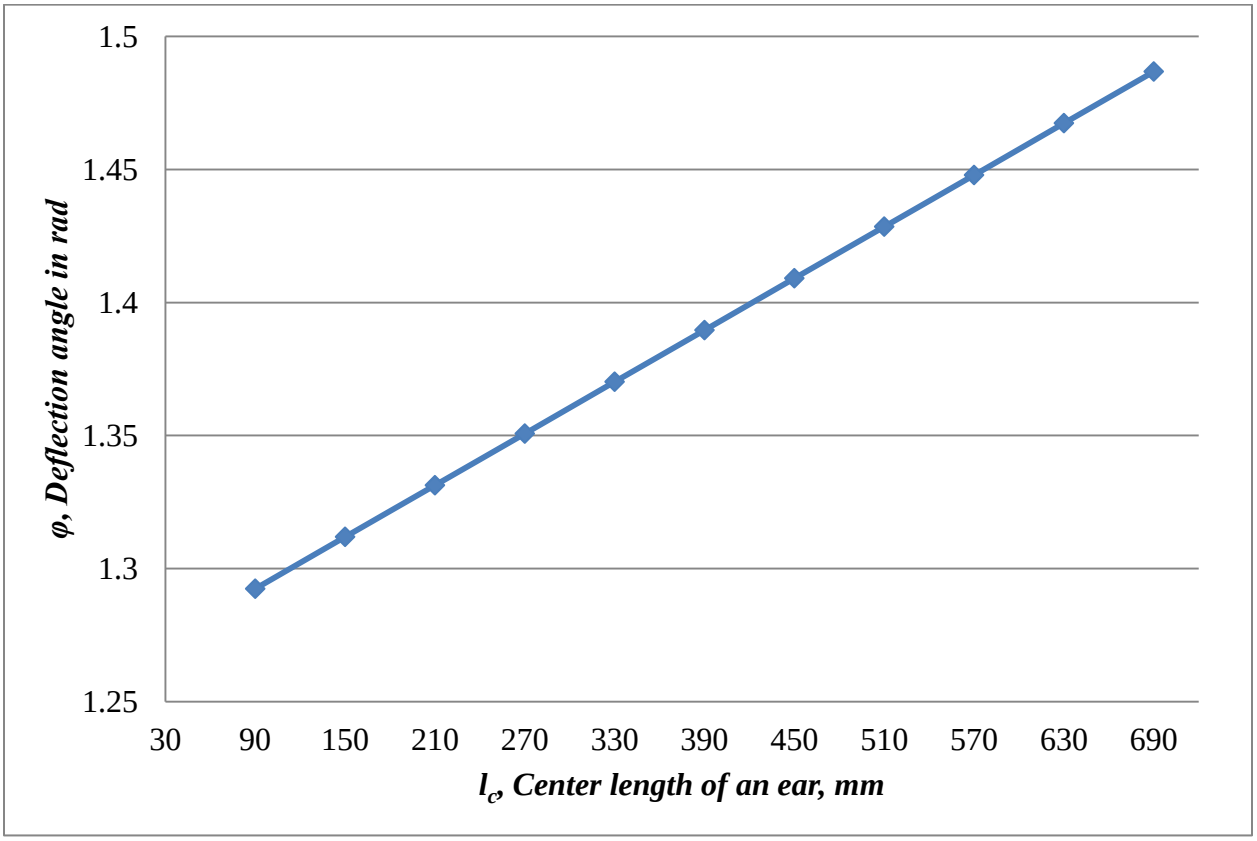

Fig. 11 Effect of center length of an ear on deflection angle, $P = 0.5\ N$, $D = 30.1\ kNmm^2$ and $W = 0.025\ N$

4.8. Relationship between reel operation and deflection of a standing crop stalk

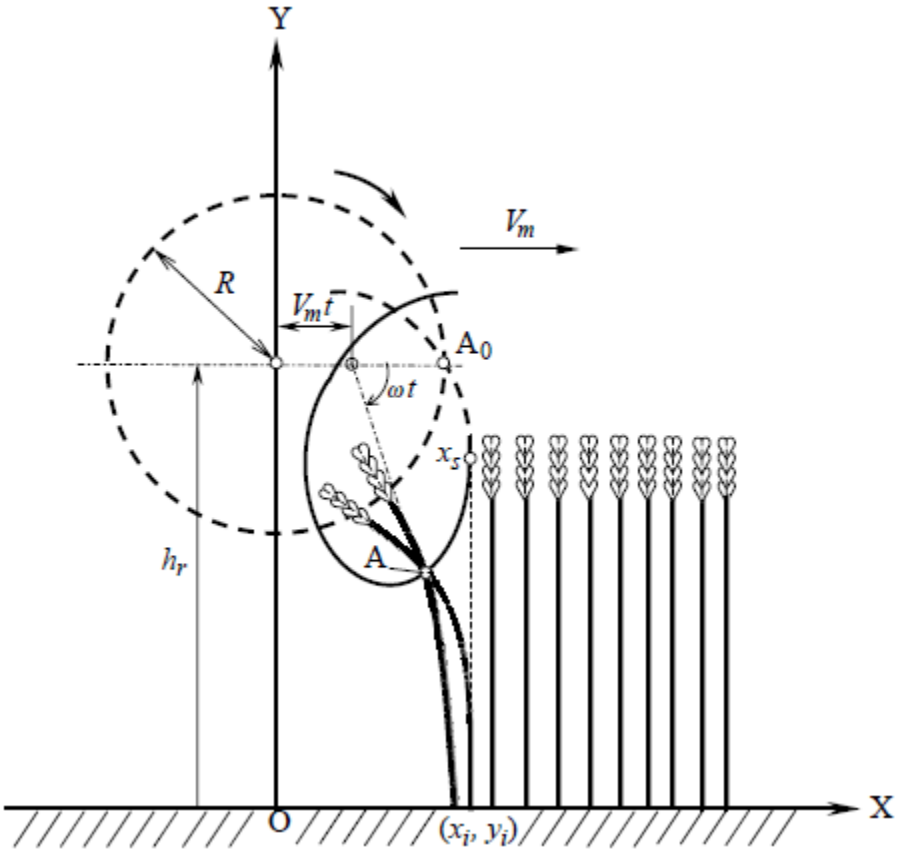

Fig. 12 Trajectory of the reel and deflection of a standing crop stalk at the reel operating point *A*, deflected position at time *t*; A_0, initial position; hr, height of the reel axis; *i*, the number of crop stalks; *R*, radius of the reel; *t*, time; V_m, forward speed of the machine; (x_i, y_i), reference coordinates of crop stalks; x_s, *x* coordinate of the first contact point of a reel and crop stalks; ω, angular velocity of the reel.

The reel has a translational motion along with the machine moving at a speed V_m and a rotational motion around its own axis given by

$$u = \omega R \qquad \text{Eqn. (4.6)}$$

Where: ω is the angular velocity of the reel and

R is the radius of the reel

When u is greater than V_m the trajectory of the reel is a trochoid. The motion equation of the trochoid is given when the origin of the coordinate is located at O, and when the X-axis is taken

in the direction of the motion of the machine with the Y-axis directed upward. Then, the current (x, y) coordinates of point A from an initial position A_0 after time t, (x_p, y_p) are as follows:

$$x_p = R\cos\omega t + V_m t$$

$$y_p = h_r - R\sin\omega t \qquad \text{Eqn. (4.7)}$$

Where: h_r is the height of the reel axis

In this case, the reel effectively feeds the crop stalks to the conveying unit (Bosoi et al., 1991).

4.9. Determination of reel stagger and appropriate number of tine bar on the reel

Application of crop stem deflection for the determination of combine harvester reel stagger denoted Z_r. The underlying postulate is that crop stems should be cut by the cutter bar at the moment when, or before, the velocity of the ascending deflecting tine bar becomes tangential to the curvature of the deflected stems. As a consequence, the following equation 4.9 was derived Oduori, (1994). In Figure 13, the vertical distance labeled R_0 is equal, in magnitude, to the reel advance per radian of rotation of the reel and expressed as: Oduori et.al, (1993)

$$R_0 = V_m/\omega \qquad \text{Eqn. (4.8)}$$

Although the unit of R_0 can be stated as meters per radian, R_0 has the dimensions of a length since the radian is a dimensionless quantity. Therefore, in mathematical expressions, R and R_0 can be treated as quantities of the same kind without violating the requirement of dimensional homogeneity.

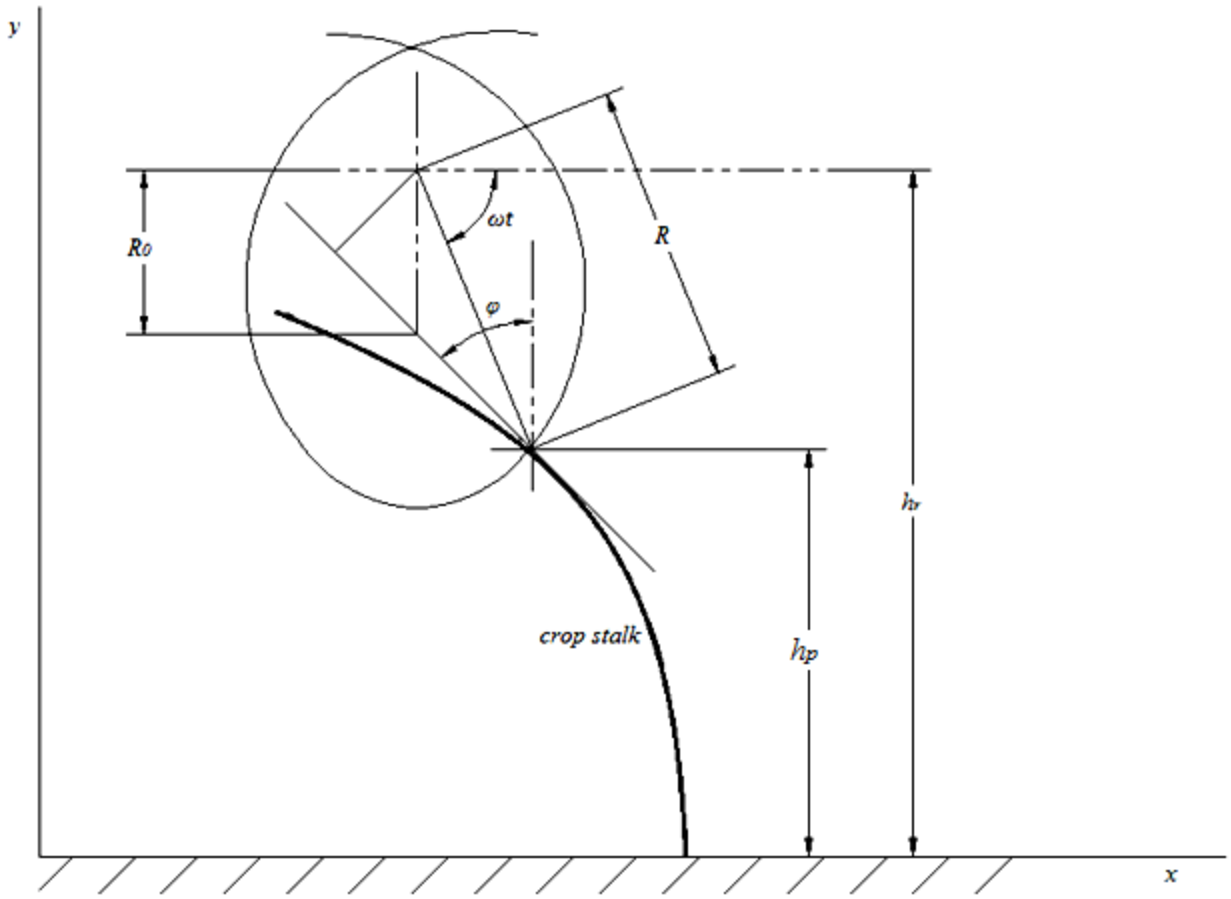

Fig. 13 Relationship between crop stalk deflection and reel kinematic parameters

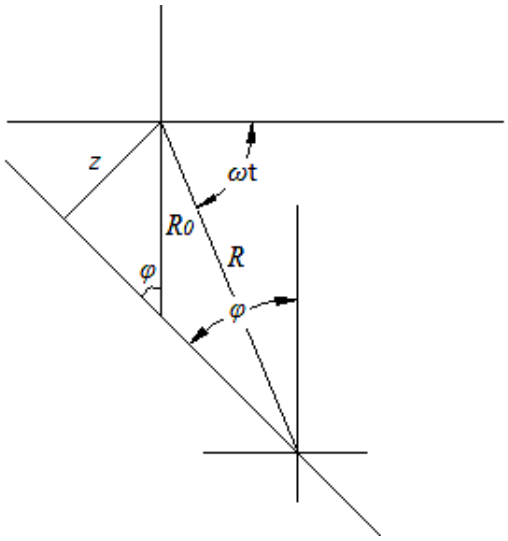

Fig. 14 Free body diagram of crop stalk deflection and reel kinematic parameters

$$z = R\sin\left[\varphi - \left(\frac{\pi}{2} - \omega t\right)\right] = R_0 \sin\varphi$$

$$R\sin\left(\omega t - \frac{\pi}{2} + \varphi\right) = R_0 \sin\varphi$$

$$\sin\left(\omega t - \frac{\pi}{2} + \varphi\right) = \frac{R_0}{R}\sin\varphi$$

$$\omega t - \frac{\pi}{2} + \varphi = \sin^{-1}\left(\frac{R_0}{R}\sin\varphi\right)$$

$$\omega t = \sin^{-1}\left(\frac{R_0}{R}\sin\varphi\right) + \frac{\pi}{2} - \varphi \qquad \text{Eqn. (4.9)}$$

Another possible application of the deflection of crop stems by the reel is in the estimation of the appropriate number, *n*, of tine bars that the reel should have. The principle is illustrated in Figure 15. The rationale is that as the stems deflected by the leading tine bar are cut the lagging tine bar should be in such a position as to support the stems that will be cut next; otherwise the possibility arises of the crop that is cut without being supported by the reel eventually being lost by falling to the ground ahead of header. In practice some stems are sandwiched between those deflected by the leading tine bar and those deflected by the lagging tine bar, but the effect of these, on the equations to be derived concerning the number of tine bars on the reel, has been neglected.

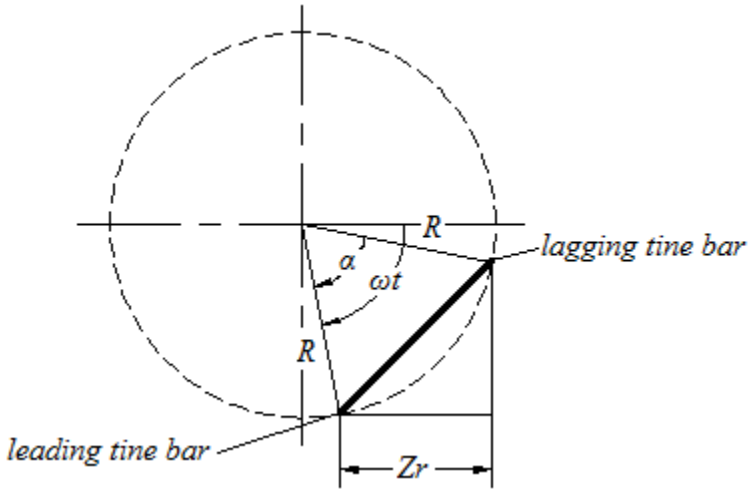

Fig. 15 Angular displacement of two successive tine bars

$$Z_r = R\cos(\omega t - \alpha) - R\cos\omega t$$

$$Z_r = R[\cos(\omega t - \alpha) - \cos\omega t]$$

$$\cos(\omega t - \alpha) - \cos\omega t = \frac{Z_r}{R}$$

$$\cos(\omega t - \alpha) = \frac{Z_r}{R} + \cos\omega t$$

$$\omega t - \alpha = \cos^{-1}\left(\frac{Z_r}{R} + \cos\omega t\right)$$

$$\alpha = \omega t - \cos^{-1}\left(\frac{Z_r}{R} + \cos\omega t\right) \qquad \text{Eqn. (4.10)}$$

Furthermore, the number of tine bars on the reel can be calculated as follows:

$$n = \frac{2\pi}{\alpha} \qquad \text{Eqn. (4.11)}$$

4.10. Reel stagger and angular displacement between successive tine bars

By solving eqn. (4.10), taking the angular displacement of the reel and radius of reel as constant values, calculating angular displacement between successive tine bars by varying reel stagger yields values below in the graph. The angular displacement between successive tine bars increased with varying reel stagger as shown in figure 16.

However, the number of tine bars on the reel decreased with angular displacement of successive tine bars increase.

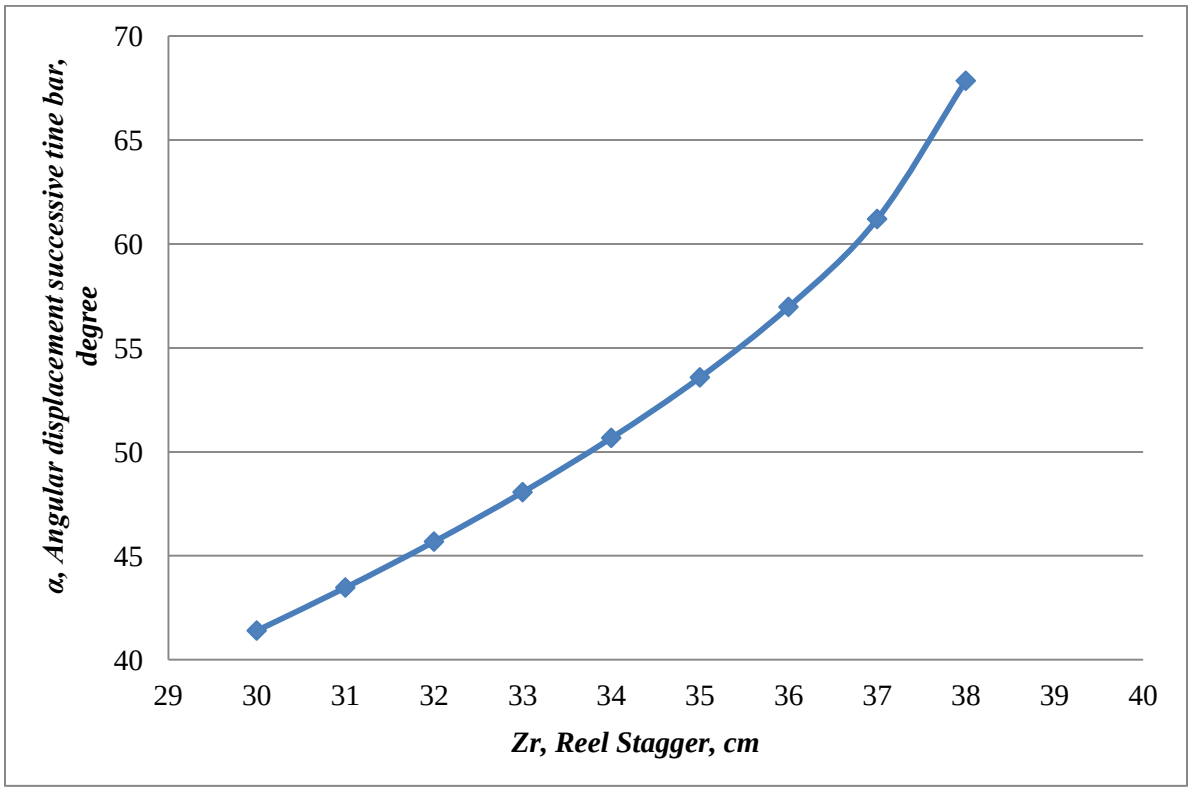

Fig. 16 Effect of reel stagger on angular displacement of successive tine bar, radius of reel $R = 53\ cm$ and deflection angle of tef crop $\varphi = 54^o$

5. Design and development of combine harvester reel

5.1. Design of reel

5.1.1. Determination of deflection angle

Input Data

X coordinate at acting point of concentrated load, l_c = 330 mm

Length of crop, *L* = 800 mm

Height at the loading point, h_p = 390 mm

Reel force P = 0.5 N

Flexural rigidity D = 30.1 kN.mm^2

Weight of ear W = 0.025 N

Deflection Angle φ calculated by eqn. (4.4) in MATLAB computer program:

$$\varphi = 1.3702\ rad\ \ or\ 54^o$$

The above input data selected by average and appropriate values

5.1.2. Determination of angular displacement of successive tine bar

To determine the number of tine bars on the reel based on deflection angle and reel stagger.

Input data

Deflection angle φ = 54^o

Reel radius *R* = 53 cm

Reel rotational speed 39 rpm

Reel stagger *Zr* = 38 cm

Rotational velocity of the reel

$$\omega = \frac{2\pi N}{60} = \frac{2\pi \times 39}{60} = 4.08\ rad/s$$

Peripheral speed of the reel

$$u = \omega R = 4.08 \times 53 = 216.45\ cm/s = 2.16\ m/s$$

Forward speed of the machine

Reel speed index is defined as the ratio of reel peripheral speed to forward travel speed and is typically 1.25 to 1.5 under most conditions in upright crops (Kepner et al. 1978).

$$V_m = u/1.25 = 2.16/1.25 = 1.728\ m/s$$

Distance whose magnitude is equal to header advance per radian of reel rotation, *Ro*

$$R_0 = V_m/\omega = 1.728/4.08 = 0.41\ m = 41\ cm$$

By using eqn. (4.9)

$$\omega t = \sin^{-1}\left(\frac{R_0}{R}\sin\varphi\right) + \frac{\pi}{2} - \varphi$$

$$\omega t = \sin^{-1}\left(\frac{41}{53}\times \sin 54\right) + 90 - 54$$

$$\omega t = 73.89^o$$

Angular displacement α between successive tine bars calculated by eqn. (4.10)

$$\alpha = \omega t - \cos^{-1}\left(\frac{Z_r}{R} + \cos\omega t\right)$$

$$\alpha = 73.89 - \cos^{-1}\left(\frac{38}{53} + \cos 73.89\right)$$

$$\alpha = 61.11^o$$

5.1.3. Determination of number of tine bar

The number of tine bars on the reel n:

$$n = \frac{2\pi}{\alpha} = \frac{360}{61.11} = 5.89 \approx 6$$

Therefore, angular displacement of successive tine bars after the approximation in the above equation.

$$\alpha = 60^0$$

Tine adjustment

- Start the pickup reel with a pitch adjustment of about 5 degrees
- Too much pitch causes the cut crop to wind around the pickup reel because the tines do not release the crop.

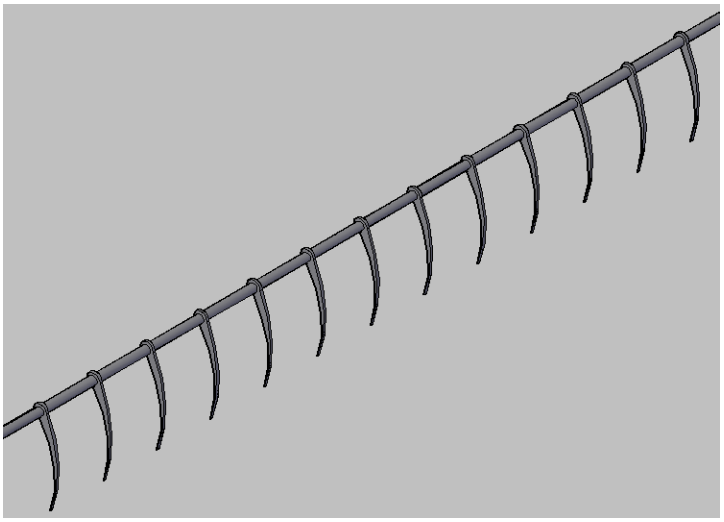

Fig. 17 Tine bar

Reel position adjustment

- Height of reel adjust by rotate at fix point

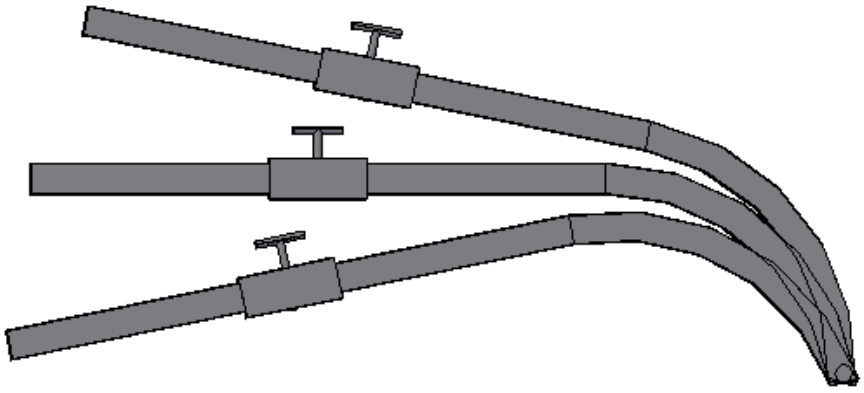

Fig. 18 Height of reel adjustments

- Forward and backward adjustment by sliding movement along the supporter arms

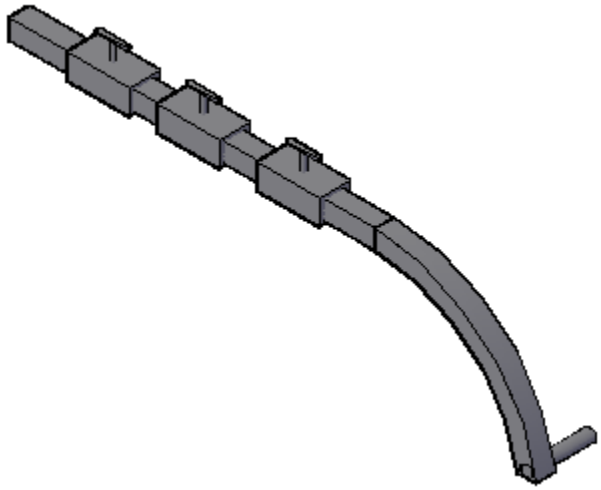

Fig. 19 Forward and backward reel adjustments

Principal stress of reel arm under different reel weight position

- Reel arm material is carbon steel

  Young's modulus 207 GPa
- Reel weight W = 4452 N
- Shaft weight W = 2054 N

  Unit weight of carbon steel 76.5 kN/m^3 (Appendix A) and volume = 0.0343 m^3

  Cross section of reel arm

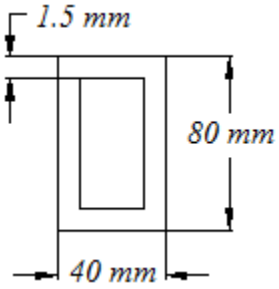

1st principal stress on reel arm, when applied weight in the left side is 322 MPa and right side is 147 MPa. These stresses are less than ultimate stress of carbon steel 500 MPa from Table 7.

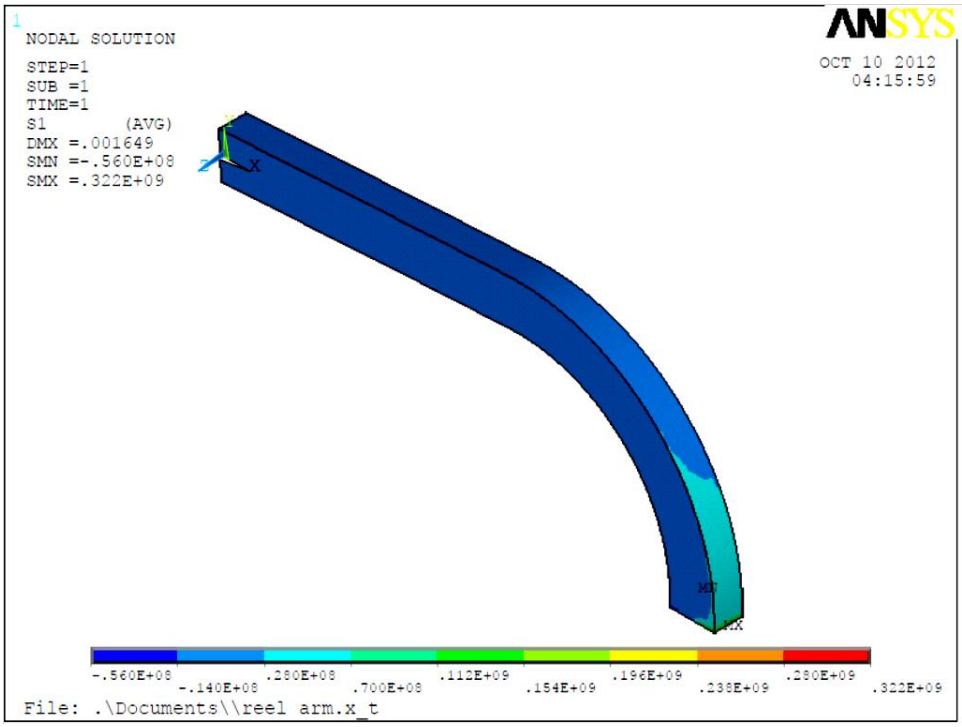

Fig. 20 1st principal stress on reel arm, when weight in the left side

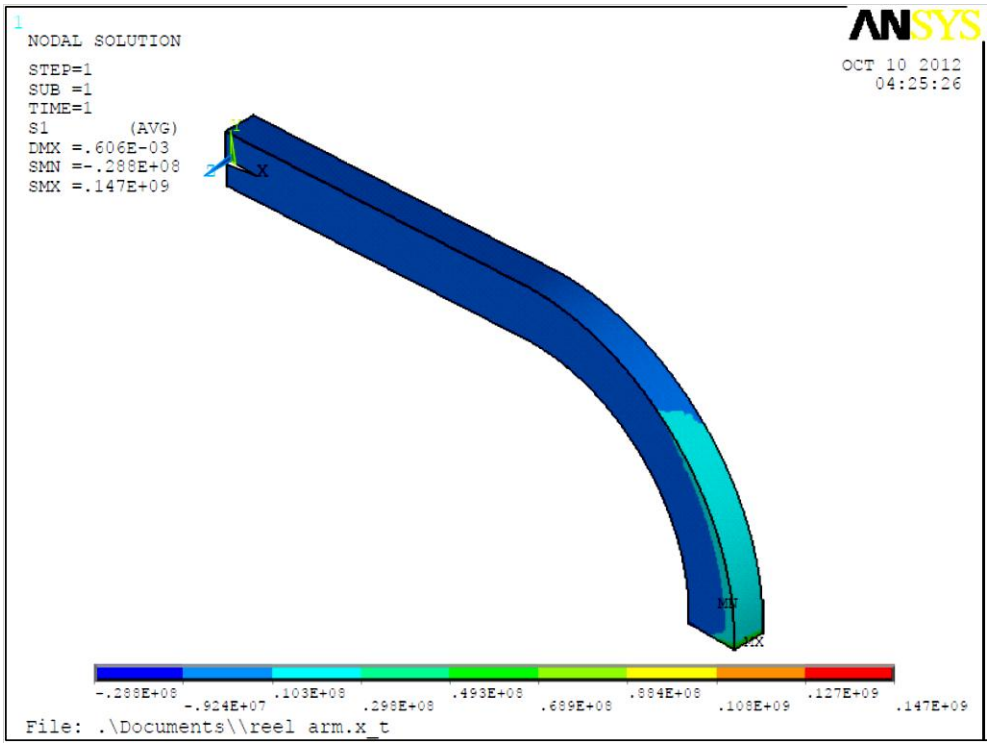

Fig. 21 1st principal stress on reel arm, when weight in the right side

5.2. Chain Drives Design

The chains are made up of number of rigid links which are hinged together by pin joints in order to provide the necessary flexibility for wrapping round the driving and driven wheels and also avoid slipping. These wheels have projecting teeth of special profile and fit into the corresponding recesses in the links of the chain. The toothed wheels are known as sprocket wheels or simply sprockets. The sprockets and the chain are thus constrained to move together without slipping and ensures perfect velocity ratio.

The chains are mostly used to transmit motion and power from one shaft to another, when the centre distance between their shafts is short such as in bicycles, motor cycles, agricultural machinery, conveyors, rolling mills, road rollers etc. Basic features of chain drives include a constant ratio, since no slippage or creep is involved; long life; and the ability to drive a number of shafts from a single source of power. The chains may also be used for long centre distance of up to 8 meters. The chains are used for velocities up to 25 m/s and for power up to 110 kW (Gupta and Khurmi, 2005). In some cases, higher power transmission is also possible.

The velocity ratio of a chain drive is given by

$$V.R = \frac{N_1}{N_2} = \frac{T_2}{T_1} \qquad \text{Eqn. (5.1)}$$

N_1 = Speed of rotation of smaller sprocket in rpm

N_2 = Speed of rotation of larger sprocket in rpm

T_1 = Number of teeth on the smaller sprocket

T_2 = Number of teeth on the larger sprocket

Table 2 Number of teeth on the smaller sprocket. Source: (Gupta and Khurmi, 2005)

Type of chain	*Number of teeth at velocity ratio*					
	1	2	3	4	5	6
Roller	31	27	25	23	21	17
Silent	40	35	31	27	23	19

The average velocity of the chain is given by

$$v = \frac{\pi DN}{60} = \frac{T\ p\ N}{60} \qquad \text{Eqn. (5.2)}$$

D = Pitch circle diameter of the sprocket in meter

p = Pitch of the chain in meters

$$p = D \sin\frac{180}{T}$$

$$D = p\ \text{cosec}\frac{180}{T} \qquad \text{Eqn. (5.3)}$$

The length of the chain (L) must be equal to the product of the number of chain links (K) and the pitch of the chain (p). Mathematically,

$$L = K.p \qquad \text{Eqn. (5.4)}$$

The number of chain links may be obtained from the following expression (Gupta and Khurmi, 2005)

$$K = \frac{T_1 + T_2}{2} + \frac{2x}{p} + \left[\frac{T_2 - T_1}{2\pi}\right]^2 \frac{p}{x} \qquad \text{Eqn. (5.5)}$$

The value of K as obtained from the above expression must be approximated to the nearest even number. The center distance is given by

$$x = \frac{p}{4}\left[K - \frac{T_1 + T_2}{2} + \sqrt{\left(K - \frac{T_1 + T_2}{2}\right)^2 - 8\left(\frac{T_2 - T_1}{2\pi}\right)^2}\right] \qquad \text{Eqn. (5.6)}$$

In order to accommodate initial sag in the chain, the value of the center distance obtained from the above equation should be decreased by 2 to 5 mm.

The factor of safety for chain drives is defined as the ratio of the breaking strength (W_B) of the chain to the total load on the driving side of the chain (W). Mathematically,

$$Factor\ of\ safety = \frac{W_B}{W} \qquad \text{Eqn. (5.7)}$$

The breaking strength of the chain may be obtained by the following empirical relations (Gupta and Khurmi, 2005)

$W_B = 106p^2$ (in newtons) for roller chains

$W_B = 106p$ (in newtons) per mm width of chain for silent chains

p is the pitch in mm

The tangential driving force (F_T)

$$F_T = \frac{Power\ transmitted\ (in\ watts)}{Speed\ of\ chain\ in\ m/s} = \frac{P}{v}\ (in\ newtons) \qquad \text{Eqn. (5.8)}$$

The power transmitted by the chain on the basis of breaking load is given by

$$P = \frac{W_B \times v}{n \times K_S} \qquad \text{Eqn. (5.9)}$$

$W_B =$ Breaking load in newtons

$v =$ Velocity of chain in m/s

$n =$ Factor of safety

$K_S =$ Service factor $= K_1.K_2.K_3$

The service factor (K_S) is the product of various factors, such as load factor (K_1), lubrication factor (K_2) and rating factor (K_3). The values of these factors are taken as follows (Gupta and Khurmi, 2005):

1. Load factor (K_1) = 1, for constant load
   = 1.25, for variable load with mild shock
   = 1.5, for heavy shock loads
2. Lubrication factor (K_2) = 0.8, for continuous lubrication
   = 1, for drop lubrication
   = 1.5, for periodic lubrication
3. Rating factor (K_3) = 1, for 8 hours per day
   = 1.25, for 16 hours per day
   = 1.5, for continuous service

The power rating for simple roller chains depending upon the speed of the smaller sprocket is shown in the following table.

Table 3 Power rating (in kW) of simple roller chain. Source: (Gupta and Khurmi, 2005)

Speed of smaller sprocket or opinion (rpm)	*Power (kW)*				
	06 B	08 B	10 B	12 B	16 B
100	0.25	0.64	1.18	2.01	4.83
200	0.47	1.18	2.19	3.75	8.94
300	0.61	1.70	3.15	5.43	13.06
500	1.09	2.72	5.01	8.53	20.57
700	1.48	3.66	6.71	11.63	27.73
1000	2.03	5.09	8.97	15.65	34.89
1400	2.73	6.81	11.67	18.15	38.47
1800	3.44	8.10	13.03	19.85	-
2000	3.80	8.67	13.49	20.57	-

Table 4 Factor of safety (n) for bush roller and silent chains. Source: (Gupta and Khurmi, 2005)

Type of chain	*Pitch of chain (mm)*	*Speed of the sprocket pinion in rpm*								
		50	200	400	600	800	1000	1200	1600	2000
Bush roller chain	12 – 15	7	7.8	8.55	9.35	10.2	11	11.7	13.2	14.8
	20 – 25	7	8.2	9.35	10.3	11.7	12.9	14	16.3	-
	30 – 35	7	8.55	10.2	13.2	14.8	16.3	19.5	-	-
Silent chain	12.7 – 15.87	20	22.2	24.4	28.7	29.0	31.0	33.4	37.8	42.0
	19.05 – 25.4	20	23.4	26.7	30.0	33.4	36.8	40.0	46.5	53.5

Input Data for chain drive design:

The reel maximum torque 1000 Nm

Reel rotational speed 39 rpm

The reel operates 16 hours per day

Power supply in smaller sprocket 4.084 kW at 100 rpm

The velocity ratio of chain drive

$$V.R = \frac{N_1}{N_2} = \frac{100}{39} = 2.56 \approx 3$$

From Table 2, we find that for the roller chain, the numbers of teeth on the smaller sprocket or pinion (T_1) for a velocity ratio of 3 are 25.

Number of teeth on the larger sprocket or gear,

$$T_2 = T_1 \times \frac{N_1}{N_2} = 25 \times \frac{100}{39} = 64.1 \approx 64$$

Now, the design power

$$Design\ Power = Rated\ Power \times Service\ factor\ (K_S)$$

The service factor (K_S) is the product of various factors K_1, K_2 and K_3. The values of these factors are taken as follows:

Load factor (K_1) for variable load with load with mild shock $= 1.25$

Lubrication factor (K_2) for drop lubrication $= 1$

Rating factor (K_3) for 16 hours per day $= 1.25$

$\therefore Service\ factor, \quad K_S = K_1.K_2.K_3 = 1.25 \times 1 \times 1.25 = 1.5625 \quad and$

$Design\ Power = 4.084 \times 1.5625 = 6.38\ kW$

From Table 3, we find that corresponding to a pinion speed of 100 rpm the power transmitted for chain No. 16 is 4.83 kW per strand. Therefore, a chain No. 16 with single strands can be used to transmit the required power. Form Table 5, we find that

Pitch, $p = 25.4\ mm$

Roller diameter, $d = 15.88\ mm$

Minimum width of roller, $w = 17.02\ mm$

Breaking load, $W_B = 42.3\ kN = 42.3 \times 10^3\ N$

Table 5 Characteristics of roller chains according to IS: 2403 — 1991.

ISO chain number	*Pitch (p) mm*	*Roller diameter (d_1) mm Maximum*	*Width between inner plates (b_1) mm Maximum*	*Transverse pitch (p_t) mm*	*Breaking load (kN) Minimum*		
					Simple	*Duplex*	*Triplex*
05 B	8.00	5.00	3.00	5.64	4.4	7.8	11.1
06 B	9.525	6.35	5.72	10.24	8.9	16.9	24.9
08 B	12.70	8.51	7.75	13.92	17.8	31.1	44.5
10 B	15.875	10.16	9.65	16.59	22.2	44.5	66.7
12 B	19.05	12.07	11.68	19.46	28.9	57.8	86.7
16 B	25.4	15.88	17.02	31.88	42.3	84.5	126.8
20 B	31.75	19.05	19.56	36.45	64.5	129	193.5
24 B	38.10	25.40	25.40	48.36	97.9	195.7	293.6
28 B	44.45	27.94	30.99	59.56	129	258	387
32 B	50.80	29.21	30.99	68.55	169	338	507.10
40 B	63.50	39.37	38.10	72.29	262.4	524.9	787.3
48 B	76.20	48.26	45.72	91.21	400.3	800.7	1201

Pitch circle diameter of the smaller sprocket or pinion,

$$d_1 = p\,\text{cosec}\left(\frac{180}{T_1}\right) = 25.4\,\text{cosec}\left(\frac{180}{25}\right) = 203\ mm = 0.203\ m$$

and pitch circle diameter of the larger sprocket or gear

$$d_2 = p\,\text{cosec}\left(\frac{180}{T_2}\right) = 25.4\,\text{cosec}\left(\frac{180}{64}\right) = 518\ mm = 0.518\ m$$

Pitch line velocity of the smaller sprocket,

$$v_1 = \frac{\pi d_1 N_1}{60} = \frac{\pi \times 0.203 \times 100}{60} = 1.06\ m/s$$

Therefore, load on the chain

$$W = \frac{Rated\ power}{Pitch\ line\ velocity} = \frac{4.084}{1.06} = 3.853\ kN = 3853\ N$$

$$factor\ of\ safety = \frac{W_B}{W} = \frac{42.3 \times 10^3}{3853} = 10.97$$

This value is more than the value given in Table 4 so the minimum center distance between the smaller and larger sprockets should be selected 30 to 50 times the pitch. Let us take it as 30 times the pitch.

∴ Center distance between the sprockets,

$$= 30p = 30 \times 25.4 = 762\ \text{mm}$$

In order to accommodate initial sag in the chain, the value of center distance is reduced by 2 to 5 mm.

∴ Correct center distance

$$x = 762 - 4 = 758\ \text{mm}$$

The number of chain links

$$K = \frac{T_1 + T_2}{2} + \frac{2x}{p} + \left[\frac{T_2 - T_1}{2\pi}\right]^2 \frac{p}{x}$$

$$K = \frac{25 + 64}{2} + \frac{2 \times 758}{25.4} + \left[\frac{64 - 25}{2\,\pi}\right]^2 \frac{25.4}{758}$$

$$K = 112$$

∴ Length of the chain

$$L = K.p = 112 \times 25.4 = 2852\ \text{mm} = \mathbf{2.852\ m}$$

5.3. Design of Shaft

A shaft is a rotating machine element which is used to transmit power from one place to another. The power is delivered to the shaft by some tangential force and the resultant torque (or twisting moment) set up within the shaft permits the power to be transferred to various machines linked up to the shaft. In order to transfer the power from one shaft to another, the various members such as pulleys, gears etc., are mounted on it. These members along with the forces exerted upon them causes the shaft to bend. In other words, we may say that a shaft is used for the transmission of torque and bending moment.

The standard sizes of transmission shafts are: 25 mm to 60 mm with 5 mm steps; 60 mm to 110 mm with 10 mm steps; 110 mm to 140 mm with 15 mm steps; and 140 mm to 500 mm with 20 mm steps (Gupta and Khurmi, 2005).

The material used for shafts should have the following properties:

- It should have high strength.
- It should have good machinability.
- It should have low notch sensitivity factor.
- It should have good heat treatment properties.
- It should have high wear resistant properties.

This shaft transmits power between the source and the machines absorbing power and carry machine parts such as reel, gear and bearing, therefore they are subjected to bending in addition to twisting then stresses due to combined torsional and bending loads.

When the shaft is subjected to a twisting moment (or torque) then the diameter of the shaft may be obtained by using the torsion equation.

$$T = \frac{\pi}{16} \times \tau \times d^3 \qquad \text{Eqn. (5.10)}$$

The twisting moment (T) may be obtained by using the following relation:

$$T = \frac{P \times 60}{2\pi N}$$

T = Twisting moment (Torque) acting upon the shaft

τ = Torsional shear stress

d = Diameter of shaft

P = Power transmitted (in watts) by the shaft

N = Speed of the shaft in rpm

When the shaft is subjected to a bending moment then the maximum stress (tensile or compressive) is given by the bending equation.

$$M = \frac{\pi}{32} \times \sigma_b \times d^3 \qquad \text{Eqn. (5.11)}$$

M = Bending moment

σ_b = Bending Stress

When the shaft is subjected to combined twisting moment and bending moment, then the shaft must be designed on the basis of the two moments simultaneously. Various theories have been suggested to account for the elastic failure of the materials when they are subjected to various types of combined stresses. The following theory is selected:

- Maximum normal stress theory or Rankine's theory

According to maximum normal stress theory, the maximum normal stress in the shaft,

$$\sigma_{b_{(max)}} = \frac{1}{2}\sigma_b + \frac{1}{2}\sqrt{(\sigma_b)^2 + 4\tau^2} \qquad \text{Eqn. (5.12)}$$

$$M_e = \frac{1}{2}\left[M + \sqrt{M^2 + T^2}\right] = \frac{\pi}{32} \times \sigma_b \times d^3 \qquad \text{Eqn. (5.13)}$$

The expression $\frac{1}{2}\left[M + \sqrt{M^2 + T^2}\right]$ is known as equivalent bending moment and is denoted by M_e. From this expression, diameter of the shaft (d) is obtained.

The shafts are subjected to fluctuating torque and bending moments. The combined shock and fatigue factors must be taken into account for the computed twisting moment (T) and bending moment (M). Thus for a shaft subjected to combined bending and torsion,

The equivalent twisting moment:

$$T_e = \sqrt{(K_m \times M)^2 + (K_t \times T)^2} \qquad \text{Eqn. (5.14)}$$

The equivalent bending moment:

$$M_e = \frac{1}{2}\left[K_m \times M + \sqrt{(K_m \times M)^2 + (K_t \times T)^2}\right] \qquad \text{Eqn. (5.15)}$$

K_m = Combined shock and fatigue factor for bending

K_t = Combined shock and fatigue factor for torsion.

Table 6 Recommended values for $\boldsymbol{K_m}$ *and* $\boldsymbol{K_t}$. Source: (Gupta and Khurmi, 2005)

Nature of load	K_m	K_t
1. Stationary shafts		
a. Gradually applied load	1.0	1.0
b. Suddenly applied load	1.5 to 2.0	1.5 to 2.0
2. Rotating shafts		
a. Gradually applied or steady load	1.5	1.0
b. Suddenly applied load with minor shocks only	1.5 to 2.0	1.5 to 2.0
c. Suddenly applied load with heavy shocks	2.0 to 3.0	1.5 to 3.0

Data for shaft design:

Reel maximum torque	Reel speed	Power supply in smaller sprocket at 100 rpm	Reel load
1000 Nm	39 rpm	4.084 kW	573 N/m

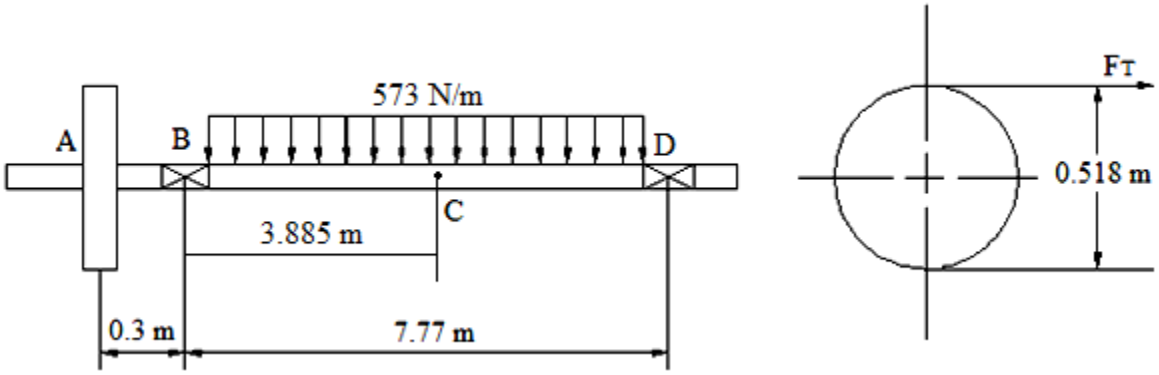

Fig. 22 Schematic diagram of forces on the shaft

For sprocket A

The tangential driving force (F_T) in horizontal load

$$F_T = \frac{Power\ transmitted\ (in\ watts)}{Speed\ of\ chain\ in\ m/s} = \frac{P}{v} = \frac{4.084}{1.06} = 3853\ N$$

Let R_{BV} and R_{CV} be the reactions at bearings B and C respectively for vertical loading. We know that

$$R_{BV} + R_{DV} = 4450\ N$$

Taking moments about *B*,

$$R_{DV} \times 7.77 = 4450 \times 3.885$$

$$R_{DV} = 2225\ N \qquad \text{and}$$

$$R_{BV} = 4450 - 2225 = 2225\ N$$

We know that B.M at *A, B* and *D*

$$M_{AV} = M_{BV} = M_{DV} = 0$$

Taking moments about *C*,

$$M_{CV} = \frac{573 \times 7.77^2}{8} = 4324.2\ Nm$$

Now considering horizontal loading, let R_{BH} and R_{CH} be the reactions at the bearings B and C respectively for horizontal loading.

$$R_{BH} + R_{DH} = 3853\ N$$

Taking moments about B,

$$R_{DH} \times 7.77 = 3853 \times 0.3$$

$$R_{DH} = 148.8\ N \qquad \text{and}$$

$$R_{BH} = 3853 - 148.8 = 3704.2\ N$$

B.M at A,

$$M_{AH} = 0$$

B.M at B,

$$M_{BH} = 3853 \times 0.3 = 1155.9\ Nm$$

B.M at C,

$$M_{CH} = 3853 \times 4.185 - 3704.2 \times 3.885 = 1733.9\ Nm$$

B.M at D,

$$M_{DH} = 3853 \times 8.07 - 3704.2 \times 7.77 = 2312\ Nm$$

The resultant bending moments for the points A, B, C and D as follows:

Resultant B.M. at $A = \sqrt{(M_{AV})^2 + (M_{AH})^2} = 0$

Resultant B.M. at $B = \sqrt{(M_{BV})^2 + (M_{BH})^2} = 1155.9\ Nm$

Resultant B.M. at $C = \sqrt{(M_{CV})^2 + (M_{CH})^2} = 4658.9\ Nm$

Resultant B.M. at $D = \sqrt{(M_{DV})^2 + (M_{DH})^2} = 2312\ Nm$

From above we see that the resultant bending moment maximum at C.

$$\therefore \qquad M = M_C = 4658.9\ Nm$$

Taking

Suddenly applied load with minor shocks only $K_m = 2\ and\ K_t = 1.5$

Bending moment $M = 4658.9\ Nm$

Maximum torque $T = 1000\ Nm$

Bending stress $\sigma_b = \sigma_e = 243\ MPa$

Equivalent bending moment,

$$M_e = \frac{1}{2}\left[K_m \times M + \sqrt{(K_m \times M)^2 + (K_t \times T)^2}\right] = \frac{1}{2}(K_m \times M + T_e)$$

$$= \frac{1}{2}\left[2 \times 4658.9 + \sqrt{(2 \times 4658.9)^2 + (1.5 \times 1000)^2}\right] = \frac{1}{2}(2 \times 4658.9 + 9437.7)$$

$$= \mathbf{9377.8\ Nm = 9377.8 \times 10^3\ Nmm}$$

Table 7 Mechanical properties of shaft materials. Source: (Richard et al., 2008)

Steel	σ_{ut}	σ_y	σ_e
Hot rolled structure steel,	410MPa	250MPa	207MPa
Grade 250 to As3679,			
Common shafting materials			
Bright steel As 1443			
Black steel As 1442			
-CS1020	400MPa	200MPa	180MPa
-CS 1030	500MPa	250MPa	225MPa
-CS 1040	540MPa	270MPa	243MPa

To get the value of shaft diameter

$$9377.8 = \frac{\pi}{32} \times \sigma_b \times d^3 = \frac{\pi}{32} \times 243 \times 10^6 \times d^3$$

$$\boldsymbol{d = 0.0732\ m = 73.2\ mm\ \approx 75\ mm}$$

Carbon Steels 1040

- 1040 steel has higher (0.40%) carbon content for greater strength than the lower carbon alloys. It is hardenable by heat treatment, quench and tempering to develop 150 to 250 ksi tensile strength.
- Machinability is good, rated at 60% that of the 1112 alloy used as a 100% machining rated steel.

By using Goodman Criterion to check the shaft is safe or not

$$\left(\frac{\sigma}{\sigma_e'}\right)^2 + \left(\frac{\tau}{\sigma_y}\right)^2 = 1$$

First determine σ and τ

$$\sigma = \frac{32M}{\pi d^3} = \frac{32 \times 4658.9}{\pi \times 0.08^3} = 112.48\ MPa$$

$$\tau = \frac{16T}{\pi d^3} = \frac{16 \times 1000}{\pi \times 0.08^3} = 12.07\ MPa$$

Determine σ_e'

$$\sigma_e' = C_S C_R \sigma_e = 0.814 \times 0.81 \times 270 = 178.14\ MPa$$

For diameters less than 250 mm (D in mm) $C_S = 1.85D^{-0.19} = 0.814$; Reliability factors, C_R from Table 8 and σ_y, CS 1040 from Table 7

Substitute in Goodman Criterion

$$\left(\frac{112.48}{178.14}\right)^2 + \left(\frac{12.07}{270}\right)^2 = 0.4 < 1 \quad shaft\ design\ is\ safe$$

Table 8 reliability factors C_R. Source: (Richard el al., 2008)

Desired reliability	Reliability factor, C_R
0.50	1.00
0.90	0.90
0.99	0.81
0.999	0.75

Stress on shaft

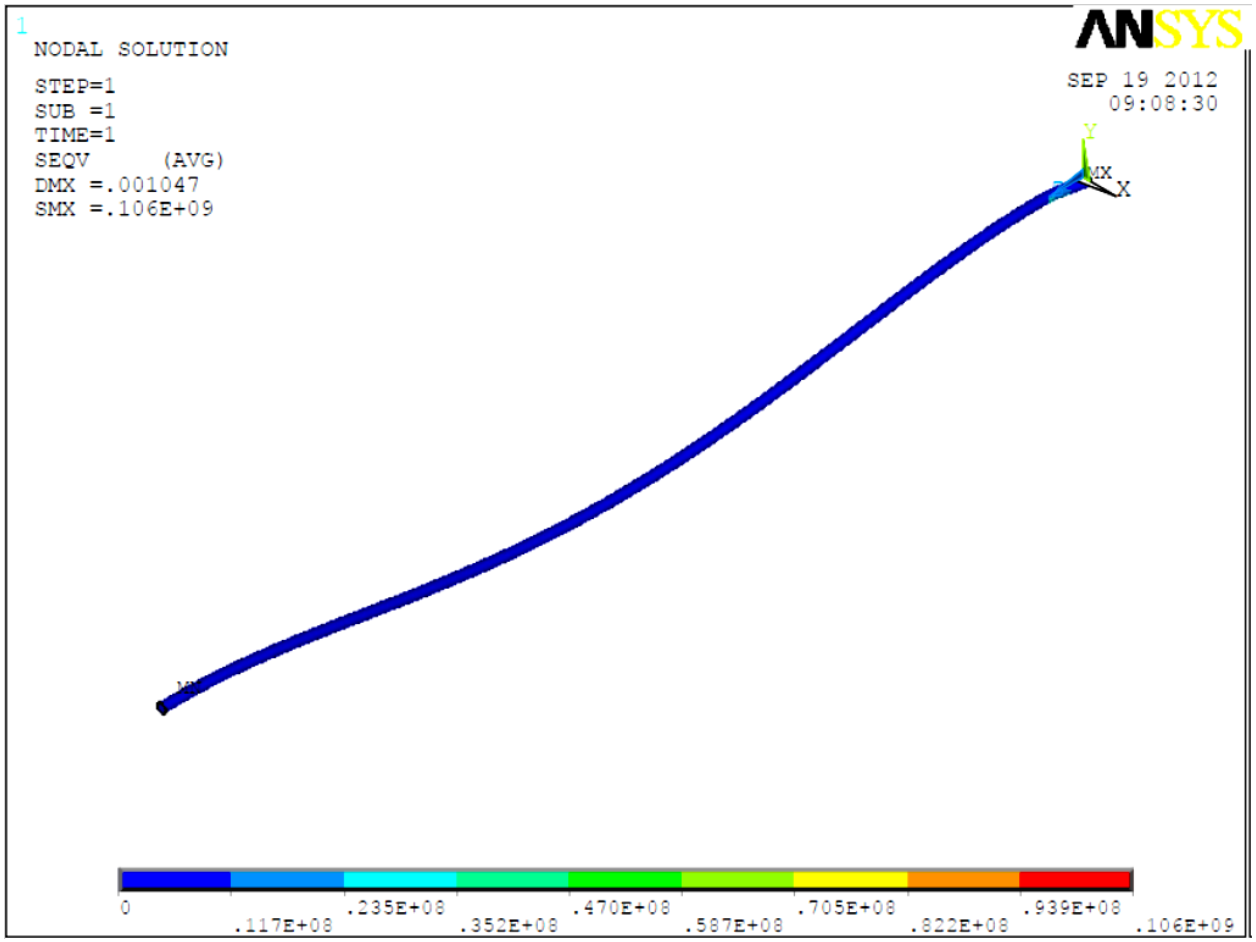

Fig. 23 von Mises Stress by contour plot

Stress

$$\sigma = \frac{32M}{\pi d^3} = \frac{32 \times 4658.9}{\pi \times 0.08^3} = 112.48\ MPa$$

Ansys: von Mises Stress $\sigma = 106\ MPa$

Theoretical: $\sigma = 112\ MPa$

5.4. Rolling contact bearing selection

The deep groove ball bearings are selected due to their high load carrying capacity and suitability for high running speeds. The load carrying capacity of a ball bearing is related to the size and number of the balls.

5.4.1. Basic dynamic load rating of rolling contact bearings

The basic dynamic load rating is defined as the constant stationary radial load (in case of radial ball or roller bearings) or constant axial load (in case of thrust ball or roller bearings) which a group of apparently identical bearings with stationary outer ring can endure for a rating life of one million revolutions (which is equivalent to 500 hours of operation at 33.3 rpm) with only 10 per cent failure (Gupta and Khurmi, 2005).

The basic dynamic load rating (*C*) in newtons for ball may be obtained as according to IS: 3824 (Part 1) – 1983, the basic dynamic radial load rating for radial and angular contact ball bearings, except the filling slot type, with balls not larger than 25.4 mm in diameter, is given by

$$C = f_c(i\cos\alpha)^{0.7} Z^{2/3}.D^{1.8} \qquad \text{Eqn. (5.16)}$$

And for balls larger than 25.4 mm in diameter,

$$C = 3.647 f_c(i\cos\alpha)^{0.7} Z^{2/3}.D^{1.4} \qquad \text{Eqn. (5.17)}$$

i = Number of rows of balls in any one bearing

Z = Number of ball per row

D = Diameter of balls, in mm

α = Nominal angle of contact *i.e.* the nominal angle between the line of action of the ball load and a plane perpendicular to the axis of bearing and

f_c = A factor, depending upon the geometry of the bearing components, the accuracy of manufacture and the material used.

5.4.2. Dynamic equivalent load for rolling contact bearings

The dynamic equivalent load may be defined as the constant stationary radial load (in case of radial ball or roller bearings) or axial load (in case of thrust ball or roller bearings) which, if applied to a bearing with rotating inner ring and stationary outer ring, would give the same life as that which the bearing will attain under the actual conditions of load and rotation.

The dynamic equivalent radial load (W) for radial and angular contact bearings, except the filling slot types, under combined constant radial load (W_R) and constant axial or thrust load (W_A) is given by

$$W = X.V.W_R + Y.W_A \qquad \text{Eqn. (5.18)}$$

$V = A$ rotation factor

$= 1$, for all types of bearings when the inner race is rotating

$= 1$, for self-aligning bearings when inner race is stationary

$= 1.2$, for all types of bearings except self-aligning when inner race is stationary

The values of radial load factor (X) and axial or thrust load factor (Y) for the dynamically loaded bearings may be taken from the following table:

Table 9 Values of service factor (K_S)

S.No.	*Type of service*	*Service factor (K_S) for radial ball bearings*
1.	Uniform and steady load	1.0
2.	Light shock load	1.5
3.	Moderate shock load	2.0
4.	Heavy shock load	2.5
5.	Extreme shock load	3.0

5.4.3. Life of a Bearing

The life of an individual ball (or roller) bearing may be defined as the number of revolutions (or hours at some given constant speed) which the bearing runs before the first evidence of fatigue develops in the material of one of the rings or any of the rolling elements.

The rating life of a group of apparently identical ball or roller bearings is defined as the number of revolutions (or hours at some given constant speed) that 90 per cent of a group of bearings will complete or exceed before the first evidence of fatigue develops (*i.e.* only 10 per cent of a group of bearings fail due to fatigue).

The term minimum life is also used to denote the rating life. It has been found that the life which 50 per cent of a group of bearings will complete or exceed is approximately 5 times the life which 90 per cent of the bearings will complete or exceed. In other words, we may say that the average life of a bearing is 5 times the rating life (or minimum life). It may be noted that the longest life of a single bearing is seldom longer than the 4 times the average life and the maximum life of a single bearing is about 30 to 50 times the minimum life. The approximate rating (or service) life of ball or roller bearing is based on the fundamental equation,

$$L = \left(\frac{C}{W}\right)^{k} \times 10^{6} \text{ revolutions}$$

$$C = W\left(\frac{L}{10^{6}}\right)^{1/k} \qquad \text{Eqn. (5.19)}$$

$L =$ Rating life

$C =$ Basic dynamic load rating

$W =$ Equivalent dynamic load and

$k = 3$, for ball bearing,

$= 10/3$, for roller bearings

The relationship between the life in revolutions (L) and the life in working hours (L_H) is given by

$$L = 60\ N.L_H\ revolutions \qquad \text{Eqn. (5.20)}$$

where N is the speed is rpm

Data for bearing design:

Reel speed 39 rpm

Average life of 5 years at 16 hours per day

Moderate shock load $K_S = 2.0$

Life of the bearing in hours,

$$L_H = 5 \times 313 \times 16 = 25040\ hours \quad \ldots (Assuming\ 313\ working\ days\ per\ year)$$

Life of the bearing in revolutions,

$$L = 60 \times 39 \times 25040 = 58.59 \times 10^6\ rev$$

The basic dynamic equivalent radial load,

$$W = X.V.W_R + Y.W_A$$

First to determine the radial and axial load form the shaft design

To get radial load

Bearing load at B

$$R_{BH} = 3704.2\ N \qquad and \qquad R_{BV} = 2225\ N$$

$$R_B = 4321\ N$$

Bearing load at D

$$R_{DH} = 148.8\ N \qquad and \qquad R_{DV} = 2225\ N$$

$$R_D = 2230\ N$$

So, selected bearing radial load maximum

$$W_R = 4321\ N$$

And no axial load act on bearing $W_A = 0$

From Appendix B take for single row angular contact ball bearing, the values of radial factor (X) and thrust factor (Y) for $W_A/W_R = 0$ (which is less than $e = 1.14$) are

$$X = 1 \qquad and \qquad Y = 0$$

Since the rotational factor (V) for most of the bearings is 1,

Therefore basic dynamic equivalent radial load,

$$W = 1 \times 1.2 \times 4321 = 5185.2\ N$$

Form Table 8 take the service factor (K_S) for ball bearing is 2.5, Heavy shock load

$$W = 2.5 \times 5185.2 = 12963\ N$$

The basic dynamic load rating,

$$C = W\left(\frac{L}{10^6}\right)^{1/k} = 12963 \times \left[\frac{58.59 \times 10^6}{10^6}\right]^{1/3} = \mathbf{50.35\ kN}$$

From Appendix C, the bearing number 215 having $C = C_{10} = 52\ kN$, selected

Bearing number 215, bore 75 mm, outer diameter 130 and width 25 mm

Therefore, the shaft daimeter and bore diametre of bearing is fit.

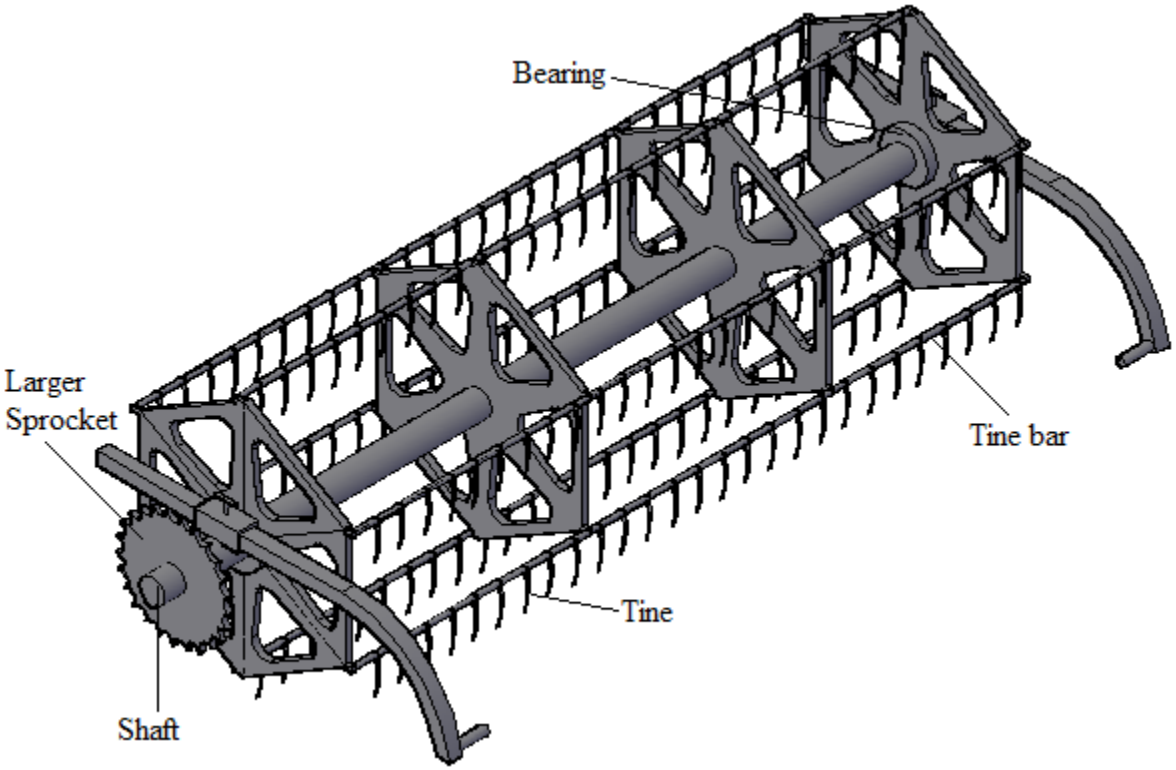

Fig. 24 Combine harvester pickup reel

5.5. Cost Analysis

Table 10 Cost of combine harvester pick up reel

No.	Items	Unit	Quantity	Unit Cost	Total Cost
1	Shaft 80 mm diameter	pcs	1	5500	5500
2	Sprocket	pcs	2	3500	7000
3	Bearing	pcs	2	200	400
4	Flat Sheet metal thickness 3 – 5 mm	sq meter	6	800	4800
5	Wire	meter	70	75	5250
6	Circular iron	meter	50	110	5500
7	Bolt and nut	pcs	12	15	180
				Overall Cost	28630 Birr

6. Conclusion and Recommendation

- The relationships between deflection angle and deflection forces of tef crop stalks were calculated using mechanical crop model and the application of the model to the reel operations, and analytical methods for determining the deflection angle and reel force.

- A model of the deflection of a crop stem as caused by the reel of a combine harvester was developed. Mathematical relations derived from the model have been evaluated against empirical data that were acquired through calculation of the deflection of the stems of a tef crop and determination of number of tine bars on the reel.

- In reel design obtained the number of tine bar on the reel and angular displacement of successive tine bars based on the tef crop deflection angle. So, tef can be harvested by combine harvester machine like rice and wheat but experimentally determine the reel acting force on the tef crop and the rotational speed of reel.

- Design of chain derives, shaft and bearing based on the appropriate and actual combine harvester pickup reel torque, speed and weight. In chain drives design, determination of the diameter of the larger sprocket and length of chain was done. In shaft design, determined the diameter of shaft and selected material. In bearing design, determined the basic dynamic load rating and bearing number that fit the shaft diameter was done.

- The tef crop mechanical property such as flexural rigidity was not found experimentally in most of Ethiopian agricultural research centers. Hence, I used the rice and wheat flexural rigidity properties in this paper with same adjustment. I recommend the teff crop radius of curvature and flexural rigidity be experimentally determined that helps to get relative design information from the tef crop lodging properties.

Reference

Baker CJ, Berry PM, Spink JH, Sylvester-Bradley R, Griffin JM, Scott RK, Clare RW. (1998). A method for the assessment of the risk of wheat lodging. Journal of Theoretical Biology 194: 587–603.

Bosoi ES; Verniaev O V; Smirnov I I; Sultan-Shakh EG (1991). Theory, Construction and Calculations of Agricultural Machines, Vol. 2, pp 443–449. Balkema, Rotterdam

Bultosa G; Taylor J R N (2004). Tef. In: Encyclopaedia of Grain Science, Eds. Wrigley, C; Corke H; Walker C; pp 253–262, Elsevier, Amsterdam

Crook MJ, Ennos AR. (1994). Stem and root characteristics associated with lodging resistance in four winter wheat cultivars. Journal of Agricultural Science 123: 167–174.

CSA (Central Statistics Authority) (1999). Agricultural Sample Survey 1998/99. Volume I: Report on area and production for major crops, Addis Abeba.

Dawit Tadesse and Hirut Kebede (1995). Germplasm collection, conservation and characterization of tef. Plant Genetic Resources Centre/Ethiopia. Internal Report. Addis Abeba, Ethiopia

Hirai Y; Inoue E; Mori K; Hashiguchi K (2002a). Investigation of mechanical interaction between a combine harvester reel and crop stalks. Biosystems Engineering, 83(3), 307–317

Hirai Y; Inoue E; Mori K; Hashiguchi K (2002b). Analysis of reaction forces and posture of a bunch of crop stalks during reel operations of a combine harvester. The CIGR Journal of Scientific Research and Development, IV, FP 02 002

Hirai Y; Inoue E; Matsui M; Mori K; Hashiguchi K (2003a). Reaction force of a wheat stalk undergoing forced displacement. Journal of the Japanese Society of Agricultural Machinery, 65(2), 47–55

Hirai Y; Inoue E; Matsui M; Mori K; Hashiguchi K (2003b). Reaction force and posture of a bunch of wheat stalks undergoing forced displacement. Journal of the Japanese Society of Agricultural Machinery, 65(2), 56–63

Inoue E; Kim Y K; Hashiguchi K; Okayasu T; Kashima J (1998). Inekan no rikigaku tokuseini kansuru ichi kousatsu. [Mechanical characteristics of rice stalk.] Journal of the Japanese Society of Agricultural Machinery, 60(2), 145–150

John Case; A.H. Chilver; Carl T.F. Ross. (1999). Strength of materials and structures, fourth edition, Arnold, a member of the Hodder Headline Group, London, Great Britain.

Kepner, R.A., R. Bainer and E.L. Barger. (1972). Principles of Farm Machinery, 3rd edition. Westport, CT: AVI Publishing Company Inc.

Klenin, N.I., I.F. PoPov and V.A. Sakun. (1970). Agricultural Machines, Theory of Operations, Computation of Controlling Parameters and the Conditions of Operations, 279-288. Translated by A. Jagnmohan Amerind Publishing Co., New Delhi.

Pinthus MJ. (1974). Lodging in wheat, barley, and oats: the phenomenon, its causes, and preventive measures. In: Brady NC, ed. Advances in agronomy, Vol. 25. New York, USA: Academic Press, 209–263.

Oduori, M. F., J. Sakai, and E. Inoue. (1993). Combine harvester reel stagger II: empirical study on crop stem deflection and application of the results for reel stagger determination. *Agricultural Mechanization in Asia, Africa and Latin America*, 24(4): 33-39.

Oduori, M. F. (1994). *Basic Principles of Combine Harvester Reel Design and Operation*. An Unpublished Ph. D. Thesis. Fukuoka, Japan: Kyushu University.

Ponti, J.A. (1978). The systematics of *Eragrostis tef* (Graminae) and related species. PhD Thesis, University of London, London, UK.

Richard G. Budynas; J. Keith Nisbett (2008). Shigley's mechanical engineering design, ninth edition, Published by McGraw-Hill, a business unit of The McGraw-Hill Companies, Inc., New York, Americas

Richey, C.B., ed. (1961). Agricultural Engineers' Handbook, 238-240. New York: McGraw-Hill.

R.S. Khurmi; J.K. Gupta (2005). A textbook of machine design: Eurasia Publishing House (PVT.) LTD Ram Nagar, New Delhi, India. pp 509 – 557, 759 – 775, 996 – 1020

Seyfu Ketema (1997). Tef *(Eragrostis tef):* breeding, genetic resources, agronomy, utilization and role in Ethiopian agriculture. Institute of Agricultural Research, Addis Abeba, Ethiopia.

Spaenij-Dekking L, Kooy-Winkelaar Y, Koning F (2005). The Ethiopian cereal tef in celiac disease. New England J. Med. 353: 16.

Srivastava A K; Goering C E; Rohrbach R P (1993). Engineering Principles of Agricultural Machines. American Society of Agricultural Engineering, pp 414–416

Stallknecht, G.F. (1997). Teff. New Crop Fact SHEET. Purdue Univ. Center for New Crops and Plant Products Web page www.hort.purdue.edu/newcrop.

Timoshenko S. (1940). Strength of Materials: Elementary theory and problem, part I, pp 134 – 143. Dover Publications, New York

Tefera H.; Ayele M.; Assefa K. (1995). Improved varieties of tef [Eragrostis tef (Zucc.) Trotter] release of 1970 – 1995. Research Bulletin. No. 1. Debre Zeit Agricultural Research Center, Ethiopia.

Teklu Y, Tefera H. (2005). Genetic improvement in grain yield potential and associated agronomic traits of tef (Eragrostis tef). Euphytica International Journal of Plant Breeding 141: 247–254.

Tulema B, Zapata F, Aune J, Sitaula B. (2005). N fertilisation, soil type and cultivars effects on N use efficiency in tef [Eragrostis tef (Zucc.) Trotter]. Nutrient Cycling in Agroecosystems 71: 203–211.

Yu JK, Sun Q, Rota Ml, Edwards H, Hailu T, Sorrells ME. (2006). Expressed sequence tag analysis in tef (Eragrostis tef (Zucc) Trotter). Genome 49: 365–372.

Zewdu A.D and W. K. Solomon (2007). Moisture-dependent physical properties of tef seed, *Biosystems Engineering*, 96(1): 57-63 doi: 10.1016/j.biosystemseng. 2006.09.008

Appendix

Appendix A: Physical Constants of Materials

Material	Modulus of Elasticity E		Modulus of Rigidity G		Poisson's Ratio ν	Unit Weight w		
	Mpsi	GPa	Mpsi	GPa		lbf/in^3	lbf/ft^3	kN/m^3
Aluminum (all alloys)	10.4	71.7	3.9	26.9	0.333	0.098	169	26.6
Beryllium copper	18.0	124.0	7.0	48.3	0.285	0.297	513	80.6
Brass	15.4	106.0	5.82	40.1	0.324	0.309	534	83.8
Carbon steel	30.0	207.0	11.5	79.3	0.292	0.282	487	76.5
Cast iron (gray)	14.5	100.0	6.0	41.4	0.211	0.260	450	70.6
Copper	17.2	119.0	6.49	44.7	0.326	0.322	556	87.3
Douglas fir	1.6	11.0	0.6	4.1	0.33	0.016	28	4.3
Glass	6.7	46.2	2.7	18.6	0.245	0.094	162	25.4
Inconel	31.0	214.0	11.0	75.8	0.290	0.307	530	83.3
Lead	5.3	36.5	1.9	13.1	0.425	0.411	710	111.5
Magnesium	6.5	44.8	2.4	16.5	0.350	0.065	112	17.6
Molybdenum	48.0	331.0	17.0	117.0	0.307	0.368	636	100.0
Monel metal	26.0	179.0	9.5	65.5	0.320	0.319	551	86.6
Nickel silver	18.5	127.0	7.0	48.3	0.322	0.316	546	85.8
Nickel steel	30.0	207.0	11.5	79.3	0.291	0.280	484	76.0
Phosphor bronze	16.1	111.0	6.0	41.4	0.349	0.295	510	80.1
Stainless steel (18-8)	27.6	190.0	10.6	73.1	0.305	0.280	484	76.0
Titanium alloys	16.5	114.0	6.2	42.4	0.340	0.160	276	43.4

Appendix B: Values of X and Y for dynamically loaded bearings

Type of bearing	*Specifications*	$\frac{W_A}{W_R} \le e$		$\frac{W_A}{W_R} > e$		*e*
		X	*Y*	*X*	*Y*	
Deep groove ball bearing	$\frac{W_A}{C_0}$ = 0.025				2.0	0.22
	= 0.04				1.8	0.24
	= 0.07				1.6	0.27
	= 0.13	1	0	0.56	1.4	0.31
	= 0.25				1.2	0.37
	= 0.50				1.0	0.44
Angular contact ball bearings	Single row		0	0.35	0.57	1.14
	Two rows in tandem		0	0.35	0.57	1.14
	Two rows back to back	1	0.55	0.57	0.93	1.14
	Double row		0.73	0.62	1.17	0.86
Self-aligning bearings	Light series : for bores					
	10 – 20 mm		1.3		2.0	0.50
	25 – 35	1	1.7	6.5	2.6	0.37
	40 – 45		2.0		3.1	0.31
	50 – 65		2.3		3.5	0.28
	70 – 100		2.4		3.8	0.26
	105 – 110		2.3		3.5	0.28
	Medium series : for bores					
	12 mm		1.0	0.65	1.6	0.63
	15 – 20		1.2		1.9	0.52
	25 – 50		1.5		2.3	0.43
	55 – 90		1.6		2.5	0.39
Spherical roller bearings	For bores :					
	25 – 35 mm		2.1		3.1	0.32
	40 – 45	1	2.5	0.67	3.7	0.27
	50 – 100		2.9		4.4	0.23
	100 – 200		2.6		3.9	0.26
Taper roller bearings	For bores :					
	30 – 40 mm				1.60	0.37
	45 – 110	1	0	0.4	1.45	0.44
	120 – 150				1.35	0.41

Appendix C: Dimensions and Load Ratings for Single-Row 02-Series Deep-Groove and Angular-Contact Ball Bearings

Bearing No.	Basic capacities in kN							
	Single row deep groove ball bearing		Single row angular contact ball bearing		Double row angular contact ball bearing		Self-aligning ball bearing	
	Static (C_0)	Dynamic (C)	Static (C_0)	Dynamic (C)	Static (C_0)	Dynamic (C)	Static (C_0)	Dynamic (C)
(1)	(2)	(3)	(4)	(5)	(6)	(7)	(8)	(9)
200	2.24	4	—	—	4.55	7.35	1.80	5.70
300	3.60	6.3	—	—	—	—	—	—
201	3	5.4	—	—	5.6	8.3	2.0	5.85
301	4.3	7.65	—	—	—	—	3.0	9.15
202	3.55	6.10	3.75	6.30	5.6	8.3	2.16	6
302	5.20	8.80	—	—	9.3	14	3.35	9.3
203	4.4	7.5	4.75	7.8	8.15	11.6	2.8	7.65
303	6.3	10.6	7.2	11.6	12.9	19.3	4.15	11.2
403	11	18	—	—	—	—	—	—
204	6.55	10	6.55	10.4	11	16	3.9	9.8
304	7.65	12.5	8.3	13.7	14	19.3	5.5	14
404	15.6	24	—	—	—	—	—	—
205	7.1	11	7.8	11.6	13.7	17.3	4.25	9.8
305	10.4	16.6	12.5	19.3	20	26.5	7.65	19
405	19	28	—	—	—	—	—	—
206	10	15.3	11.2	16	20.4	25	5.6	12
306	14.6	22	17	24.5	27.5	35.5	10.2	24.5
406	23.2	33.5	—	—	—	—	—	—
207	13.7	20	15.3	21.2	28	34	8	17
307	17.6	26	20.4	28.5	36	45	13.2	30.5
407	30.5	43	—	—	—	—	—	—
208	16	22.8	19	25	32.5	39	9.15	17.6
308	22	32	25.5	35.5	45.5	55	16	35.5
408	37.5	50	—	—	—	—	—	—
209	18.3	25.5	21.6	28	37.5	41.5	10.2	18
309	30	41.5	34	45.5	56	67	19.6	42.5
409	44	60	—	—	—	—	—	—
210	21.2	27.5	23.6	29	43	47.5	10.8	18
310	35.5	48	40.5	53	73.5	81.5	24	50
410	50	68	—	—	—	—	—	—

(1)	*(2)*	*(3)*	*(4)*	*(5)*	*(6)*	*(7)*	*(8)*	*(9)*
211	26	34	30	36.5	49	53	12.7	20.8
311	42.5	56	47.5	62	80	88	28.5	58.5
411	60	78	—	—	—	—	—	—
212	32	40.5	36.5	44	63	65.5	16	26.5
312	48	64	55	71	96.5	102	33.5	68
412	67	85	—	—	—	—	—	—
213	35.5	44	43	50	69.5	69.5	20.4	34
313	55	72	63	80	112	118	39	75
413	76.5	93	—	—	—	—	—	—
214	39	48	47.5	54	71	69.5	21.6	34.5
314	63	81.5	73.5	90	129	137	45	85
414	102	112	—	—	—	—	—	—
215	42.5	52	50	56	80	76.5	22.4	34.5
315	72	90	81.5	98	140	143	52	95
415	110	120	—	—	—	—	—	—
216	45.5	57	57	63	96.5	93	25	38
316	80	96.5	91.5	106	160	163	58.5	106
416	120	127	—	—	—	—	—	—
217	55	65.5	65.5	71	100	106	30	45.5
317	88	104	102	114	180	180	62	110
417	132	134	—	—	—	—	—	—
218	63	75	76.5	83	127	118	36	55
318	98	112	114	122	—	—	69.5	118
418	146	146	—	—	—	—	—	—
219	72	85	88	95	150	137	43	65.5
319	112	120	125	132	—	—	—	—
220	81.5	96.5	93	102	160	146	51	76.5
320	132	137	153	150	—	—	—	—
221	93	104	104	110	—	—	56	85
321	143	143	166	160	—	—	—	—
222	104	112	116	120	—	—	64	98
322	166	160	193	176	—	—	—	—

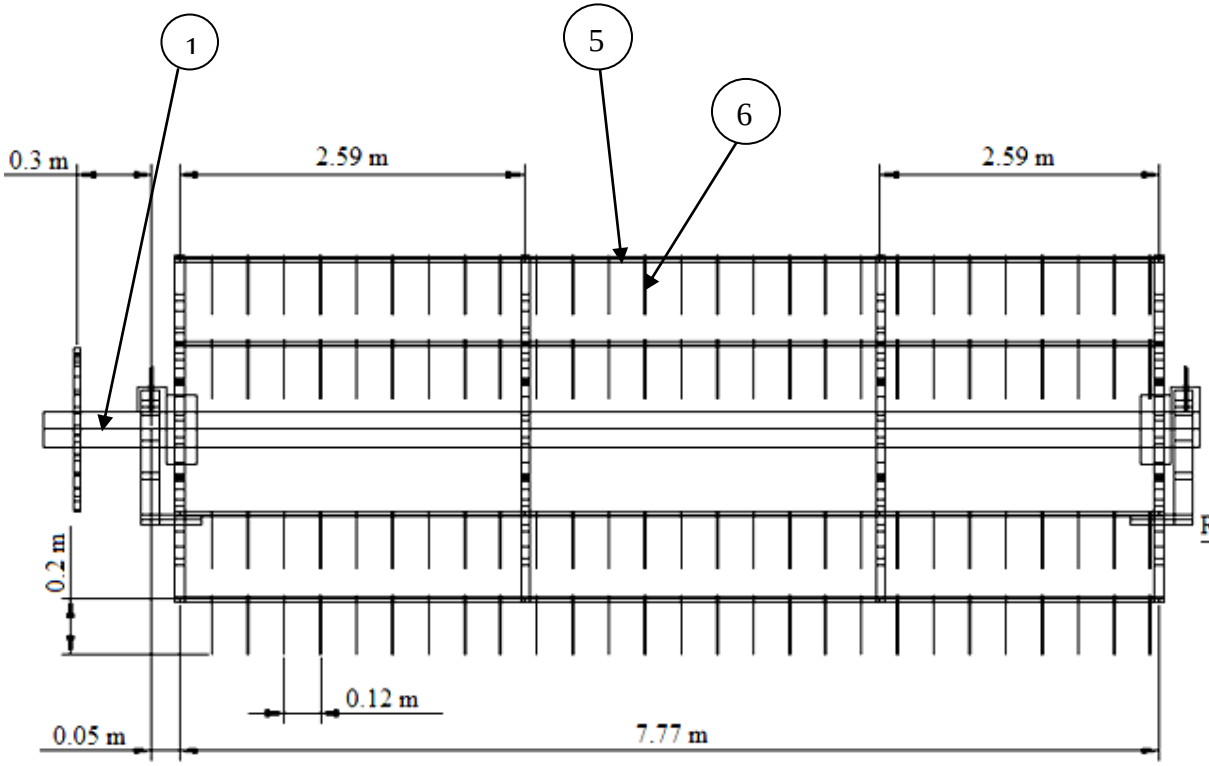

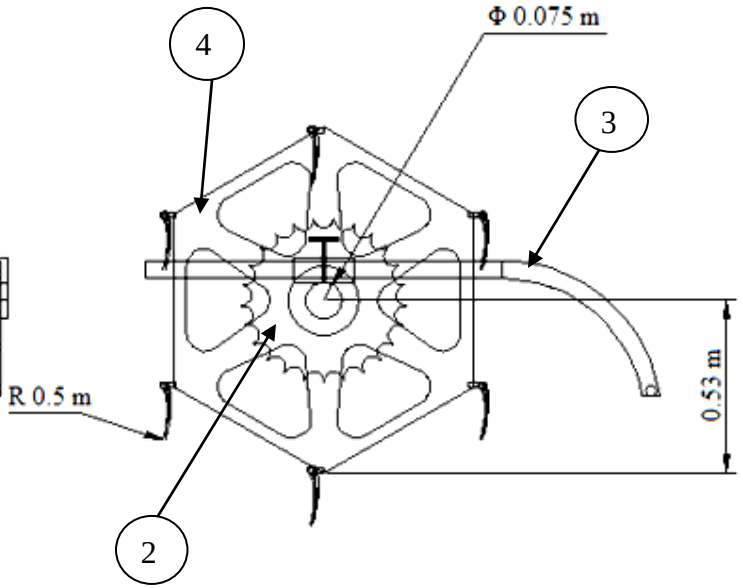

PART No.	NAME	MATERIAL	QTY.		NAME	DATE	MATL	
1	Shaft	Carbon Steel	1					
2	Sprocket	Carbon Steel	2					
3	Reel arm	Carbon Steel	2	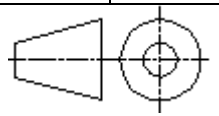			TITLE COMBINE HARVESTER PICK UP REEL	
4	Reel supporter	Carbon Steel	4					
5	Tine bar	Mild Steel	6	Scale			DRG No.	
6	Tine	Mild Steel	388					

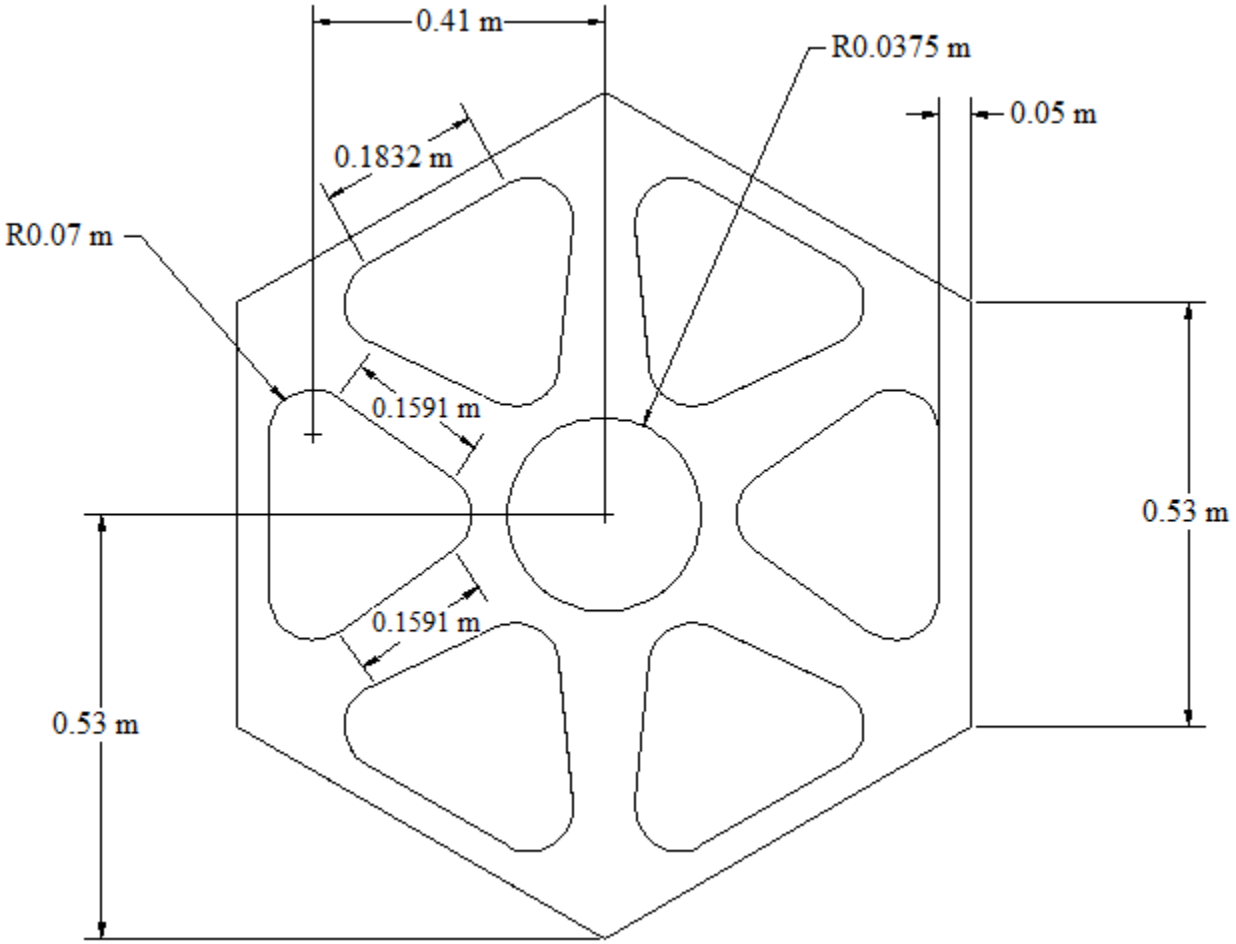

	NAME	DATE		
			CARBON STEEL	
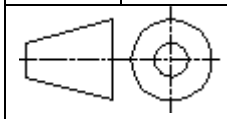			TITLE REEL SUPPORTER	
Scale			DRG No.	

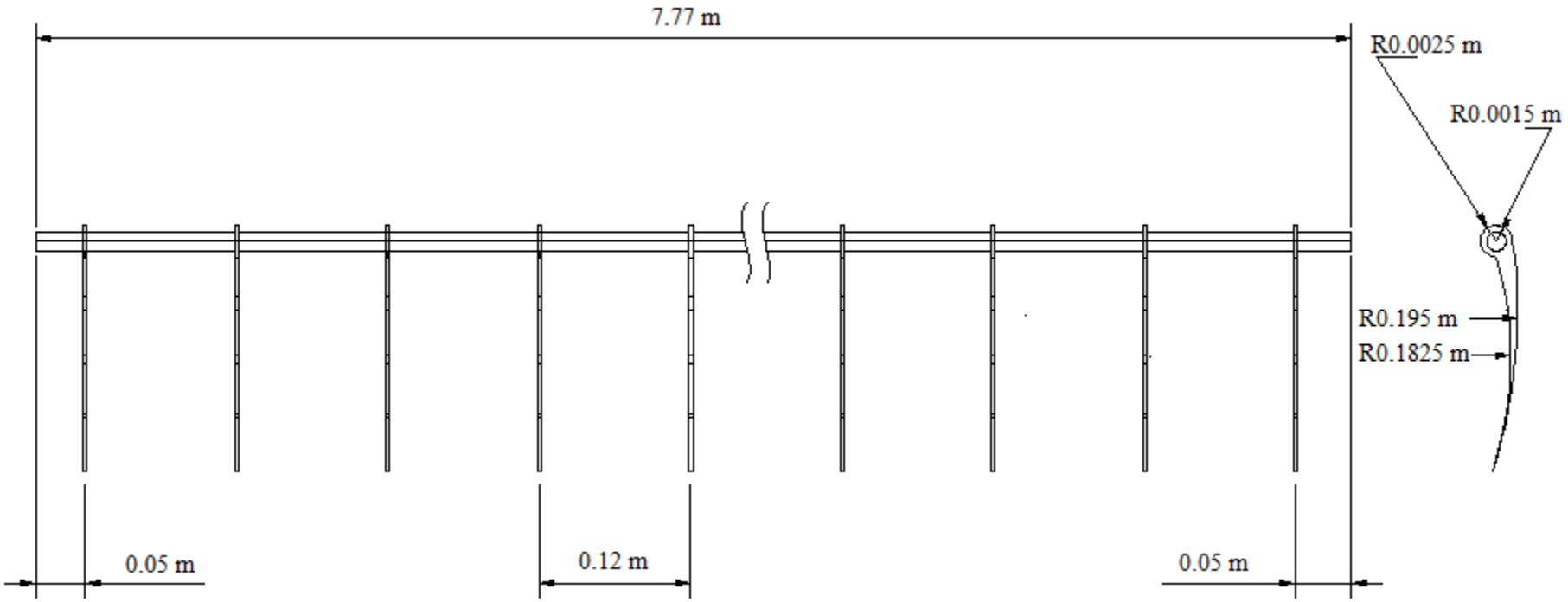

	NAME	DATE		
			MILD STEEL	
			TITLE	
			TINE BAR	
Scale			DRG No.	

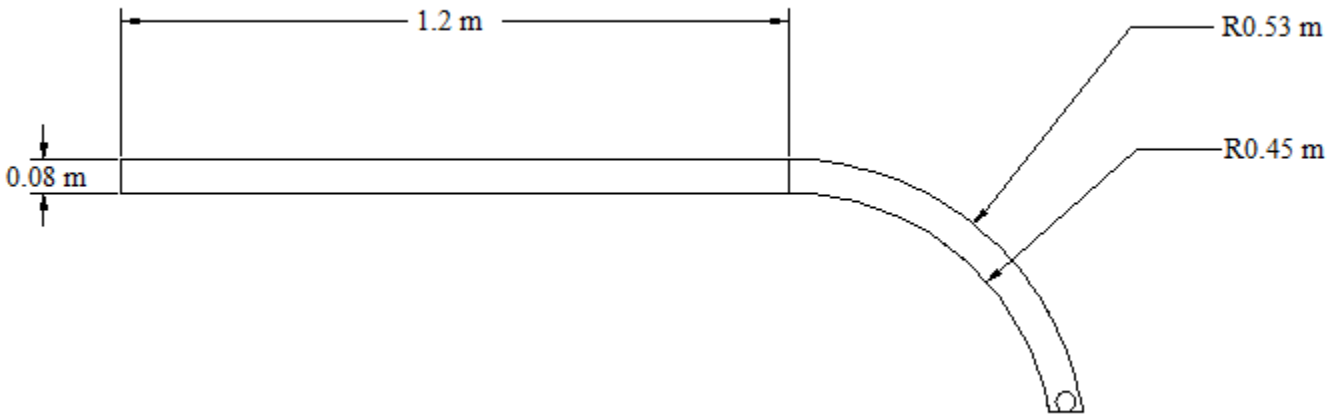

	NAME	DATE		
			CARBON STEEL	
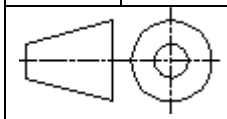			TITLE REEL ARM	
Scale			DRG No.	